



HAL
open science

IL-33 Expression Is Lower in Current Smokers at Both Transcriptomic and Protein Level

Alen Faiz, Rashad Mahbub, Fia Sabrina Boedijono, Milan Tomassen, Wierd Kooistra, Wim Timens, Martijn Nawijn, Philip Hansbro, Matt Johansen, Simon Pouwels, et al.

► **To cite this version:**

Alen Faiz, Rashad Mahbub, Fia Sabrina Boedijono, Milan Tomassen, Wierd Kooistra, et al.. IL-33 Expression Is Lower in Current Smokers at Both Transcriptomic and Protein Level. American Journal of Respiratory and Critical Care Medicine, 2023, 10.1164/rccm.202210-1881OC . hal-04249586

HAL Id: hal-04249586

<https://hal.science/hal-04249586v1>

Submitted on 19 Oct 2023

HAL is a multi-disciplinary open access archive for the deposit and dissemination of scientific research documents, whether they are published or not. The documents may come from teaching and research institutions in France or abroad, or from public or private research centers.

L'archive ouverte pluridisciplinaire **HAL**, est destinée au dépôt et à la diffusion de documents scientifiques de niveau recherche, publiés ou non, émanant des établissements d'enseignement et de recherche français ou étrangers, des laboratoires publics ou privés.

IL-33 expression is lower in current smokers at both transcriptomic and protein level

Alen Faiz^{1,2,3,†,*}, Rashad M. Mahbub^{1,†}, Fia Sabrina Boedijono^{1,5}, Milan I. Tomassen^{2,4}, Wierd Kooistra^{2,4}, Wim Timens^{2,4}, Martijn Nawijn^{2,4}, Philip M. Hansbro⁵, Matt D. Johansen⁵, Simon D. Pouwels^{2,3}, Irene H. Heijink^{2,3,4}, Florian Massip^{6,7,8}, Maria Stella de Biase⁹, Roland F. Schwarz^{9,10,11}, Cambridge Lung Cancer Early Detection Programme, Ian M. Adcock¹², Kian F. Chung¹², Anne van der Does¹³, Pieter S. Hiemstra¹³, Helene Goulaouic¹⁴, Heming Xing¹⁴, Raolat Abdulai¹⁵, Emanuele de Rinaldis¹⁵, Danen Cunoosamy¹⁵, Sivan Harel¹⁶, David Lederer¹⁶, Michael C Nivens¹⁶, Peter A. Wark^{17,18}, , Huib A.M. Kerstjens^{2,3}, Machteld N. Hylkema^{2,4}, Corry-Anke Brandsma^{2,4#}, Maarten van den Berge^{2,3#}

1. University of Technology Sydney, Respiratory Bioinformatics and Molecular Biology (RBMB), School of Life Sciences, Sydney, Australia.

2. University of Groningen, University Medical Center Groningen, Groningen Research Institute for Asthma and COPD (GRIAC), Groningen, the Netherlands.

3. University of Groningen, University Medical Center Groningen, Department of Pulmonary Diseases, Groningen, the Netherlands.

4. University of Groningen, University Medical Center Groningen, Dept of Pathology & Medical Biology Groningen, The Netherlands

5. Centre for Inflammation, Centenary Institute and University of Technology Sydney, Faculty of Science, Sydney, Australia

6. MINES ParisTech, PSL-Research University, CBIO-Centre for Computational Biology, 75006 Paris, France

7. Institut Curie, Paris, Cedex, France

8. INSERM, U900, Paris, Cedex, France
9. Berlin Institute for Medical Systems Biology, Max Delbrück Center for Molecular Medicine in the Helmholtz Association, Robert-Rössle-Str. 10, 13125 Berlin, Germany
10. Institute for Computational Cancer Biology, Center for Integrated Oncology (CIO), Cancer Research Center Cologne Essen (CCCE), Faculty of Medicine and University Hospital Cologne, University of Cologne, Germany
11. BIFOLD - Berlin Institute for the Foundations of Learning and Data, Berlin, Germany
12. National Heart & Lung Institute, Imperial College London, London SW3 6LY, UK
13. Department of Pulmonology, Leiden University Medical Center, Leiden, The Netherlands
14. Sanofi, Chilly-Mazarin, France
15. Sanofi, Cambridge, MA, USA
16. Regeneron Pharmaceuticals, Tarrytown, New York
17. The University of Newcastle, Centre for Asthma & Respiratory Disease Newcastle, NSW, AUS
18. Hunter Medical Research Institute, Vaccines, Infection, Viruses & Asthma Newcastle, NSW, AUS

Authors contributed equally

† Co-first authors

*** Corresponding author**

Alen Faiz

Email: alen.faiz@uts.edu.au

School of Life Sciences, Building 4, Room 04.07.418, University of Technology Sydney, Thomas St, Ultimo NSW 2007, Australia.

Contributions

Conception and design: AF, MvdB; Analysis and interpretation: AF, RM, FSB, MIT, CB, WT, MvdB; provided bioinformatics data: IMA, KFC, FSB, MJ, RFS, writing and reviewing the manuscript: AF, RM, FSB, MJ, SDP, MIT, AvdD, PAW, FM, RFS, MSB, IHH, MN, PSH, MvdB, MH, HK, WT, PH, CB, IMA, KFC, HX, HG, RA EdR, DC MCN, SH, DL

Funding

P.M.H. is funded by a Fellowship and grants from the National Health and Medical Research Council (NHMRC) of Australia (1079187, 1175134) and by UTS

Cancer Research UK Cambridge Centre; Cambridge NIHR Biomedical Research Centre.

This research was funded by Sanofi

RFS is a Professor at the Cancer Research Center Cologne Essen (CCCE) funded by the Ministry of Culture and Science of the State of North Rhine-Westphalia.

At a Glance Commentary

Scientific Knowledge on the Subject

IL-33 gene expression has been associated with the pathogenesis of lung diseases and human gene expression studies demonstrated between IL-33 and risk for asthma and COPD. Several studies have shown that smoking, the major risk factor for COPD, induces inflammation and influences IL-33 expression. IL-33 protein expression has been shown specific the basal cells in the airways. A previous clinical trial using the anti-IL33 antibody showed a reduction in exacerbation and improved lung function in ex-smokers but not current smokers with COPD.

What This Study Adds to the Field

We investigated the association between IL-33 levels and smoking status and whether this was related to changes to cellular composition in the airways. IL-33 gene expression and protein levels were found to be lower in current smokers compared to never/ex-smokers. While, IL-33 expression was found only in a subset of basal cells know as resting basal cells and was lost quickly after differentiation to suprabasal cells. The abundance of resting basal cells was found to be lower in during smoke exposure while suprabasal cells were higher both in-vitro and in-vivo. The current study provides evidence that the clinical observation of the greater efficacy of anti-IL-33 treatment in ex-smokers compared to current smokers with COPD may be due to the inherently lower levels of IL-33 expression in current smokers.

This article is open access and distributed under the terms of the Creative Commons Attribution Non-Commercial No Derivatives License 4.0 (<http://creativecommons.org/licenses/by-nc-nd/4.0/>). For commercial usage and reprints please contact Diane Gern (dgern@thoracic.org).

This article has an online data supplement, which is accessible from this issue's table of content online at www.atsjournals.org.

Abstract

Introduction: IL-33 is a pro-inflammatory cytokine thought to play a role in the pathogenesis of asthma and COPD. A recent clinical trial using the anti-IL33 antibody showed a reduction in exacerbation and improved lung function in ex-smokers but not current smokers with COPD. In this study, we aimed to understand the effects of smoking status on IL-33.

Methods: We investigated the association of smoking status with the level of gene expression of *IL33* in the airways in eight independent transcriptomic studies of lung airways. Additionally, we performed western blot and immunohistochemistry for IL-33 in lung tissue to assess protein levels.

Results: Across the bulk RNA-sequencing datasets, *IL-33* gene expression and its signaling pathway were significantly lower in current- compared to ex- or never-smokers and increased upon smoking cessation ($p < 0.05$). Single-cell sequencing showed that *IL-33* is predominantly expressed in resting basal epithelial cells and decreases during the differentiation process triggered by smoke exposure. We also found a higher transitioning of this cellular sub-population into a more differentiated cell type during chronic smoking, potentially driving the reduction of *IL-33*. Protein analysis demonstrated lower IL-33 levels in lung tissue from COPD current- compared to ex-smokers and a lower proportion of IL-33 positive basal cells in current versus ex-smoking controls.

Conclusion: We provide strong evidence that cigarette smoke leads to an overall reduction in IL33 expression in both transcriptomic and protein level and this may be due to the decrease in resting basal cells. Together, these findings may explain the clinical observation that a recent antibody-based anti-IL-33 treatment is more effective in ex- than current smokers with COPD.

Introduction

Chronic Obstructive Pulmonary Disease (COPD) is a highly prevalent disease characterized by progressive airflow limitation, shortness of breath, cough, and sputum production and is associated with a significant health care burden (1). Despite receiving standard-of-care treatments, including bronchodilators and anti-inflammatory therapies, a subset of COPD patients continues to experience exacerbations and accelerated decline in lung function (2). An enormous unmet need exists to identify novel, disease-modifying therapies for COPD.

Interleukin-33 (IL-33) is a member of the interleukin-1 (IL-1) family which plays an essential role in innate and adaptive immunity. It is a pro-inflammatory cytokine, or alarmin, localized in the nuclei of various cell types, including airway epithelial cells, endothelial cells, and fibroblasts which send signals to these cell types to produce inflammatory cytokines in response to infection and tissue injury(3, 4). IL-33 is rapidly released into the extracellular space following cellular damage, e.g., by exposure to viruses and cigarette smoke or air pollutants (5, 6). As a ligand, IL-33 binds to its cognate receptor, suppression of tumorigenicity 2 (ST2), also known as IL1RL1. Subsequently it engages the IL-1 receptor accessory protein (IL-1RAcP) as a co-receptor to initiate signaling and activation of downstream inflammatory pathways (6). As such, IL-33 can activate type 2 immune cells expressing high levels of ST2, e.g., Th2 cells, ILC2s, mast cells, basophils and eosinophils (5, 7). Over the years, *IL-33* gene expression has been associated with the pathogenesis of lung diseases and human gene expression studies demonstrated a clear link between *IL-33* and risk for asthma and COPD (8-10). Several studies have shown that smoking, the major risk factor for COPD, induces inflammation and influences *IL-33* expression (11-14). Moreover, lung homogenates from patients with COPD reveal that higher *IL-33* gene expression correlates with severe airflow obstruction (15).

IL-33 has been a target of therapeutic development in asthma and COPD (8, 9). In mouse studies, neutralizing IL-33 with an anti-IL-33 monoclonal antibody, Itepekimab, improved airway inflammation and tissue remodeling in a house dust mite-induced model of asthma (16). In patients with moderate-to-severe asthma, blockade of the IL-33 pathway with Itepekimab resulted in a significantly reduced proportion of patients with asthma exacerbation, and improved lung function relative to placebo (8). In another proof-of-concept clinical trial including patients with moderate-to-severe COPD, Itepekimab led to a numerical but nonsignificant annualized rate of exacerbations and significantly improved prebronchodilator FEV₁ by 60mL (9). The benefit was highest in the subgroup of ex-smokers, with a statistically significant 42% reduction of exacerbations and 90mL improvement in FEV₁. In contrast, in current smokers, there was no benefit at all in those endpoints. These findings indicate that anti-IL-33 treatment is most effective in ex-smokers, although the mechanism behind this observation remains unclear (9, 17).

In this study, we investigated the influence of smoking status on the expression of *IL-33* and its receptors, *IL1RL1* and *IL1RAP*, in bronchial biopsies and bronchial brushings to identify cellular mechanisms of differential responses to anti-IL-33 therapies between current and ex-smokers. Moreover, we assessed IL-33 protein levels as well as their splice variants in lung tissue. Some of the results of these studies have been previously reported in the form of abstracts (18, 19).

Methods

We investigated the expression of *IL33* and its receptors in eight different studies of lung airway. In five of these studies, we looked at the average gene expression (bulk RNA-sequencing or microarray), which looks at the average expression of the genes per participant.

In the other three studies, we looked at the gene expression at single-cell level (single-cell RNA-sequencing), meaning investigating the expression of IL33 and related receptors at individual cell level for each participant or sample. A brief description of the studies is given below (Figure 1, Table 1, Table S1).

Bulk RNA-sequencing/microarray studies

The STOP smoking study used RNA-sequencing to investigate the effects of smoking on gene expression in a longitudinal setting (20). The study collected bronchial biopsies from participants (n=16) before and after smoking cessation. The study aimed to identify gene expression changes that occur as a result of smoking cessation.

The GLUCOLD study used gene expression profiles from bronchial biopsies to investigate the effects of smoking on COPD (21, 22). The study collected biopsies from current (n=33) and ex-smokers (n=46) with moderate to severe COPD at a baseline time point. It is important to note that 95% were steroid naïve and 5% had no steroid in the past six months. This was conducted using microarray, while a subset was also conducted with RNA-Seq.

The COPD microarray study used a cross-sectional design to investigate gene expression changes in current (n=30) and ex-smokers (n=57) with COPD(23). The study collected large airway bronchial brush samples and used Affymetrix HG 1.0 ST Arrays to acquire gene expression profiles. The study aimed to identify specific genes and pathways that are altered in COPD due to smoking.

The NORM study aimed to compare gene expression profiles of never smokers (n=40) and current smokers (n=37)(24). The study collected bronchial brushings and biopsies from healthy never and current smokers and aimed to identify genes and pathways that are specifically affected by smoking in healthy individuals.

The CRUKPAP study recruited donors, including never smokers (n=8), ex-smokers (n=151) and current smokers (n=77) being investigated for suspicion of lung cancer (25). The study

collected bronchial brushings and used short-read total RNA sequencing to investigate gene expression changes in relation to cigarette smoking status.

Single-cell RNA-sequencing studies

We investigated one *in-vivo* and two *in-vitro* single-cell RNA-sequencing (scRNA-seq) studies to understand the transcriptomic dynamics of IL33 in response to smoke exposure. The *in-vivo* study used single-cell RNA-sequencing on the bronchial brushings of healthy current (n=6) and never smokers (n=6) (26). The COPD ALI *in-vitro* study used scRNA-seq of airway epithelial cell cultures from bronchial brushings of COPD ex- (n=2), current-smokers (n=2), and healthy never-smokers (n=3) (27). The Smoke ALI *in-vitro* study used scRNA-seq data from healthy (n=3) and COPD (n=3) small airway epithelial cells that were treated with acute (4 days) and chronic (28 days) smoke exposure (28).

Gene Expression Analysis

Differential gene expression analysis was performed on bulk RNA-seq and microarray datasets using edgeR (version 3.32.1) and limma (version 3.46.0) packages, respectively (29-31). These analyses were corrected for age and gender. Pathway analysis, cellular deconvolution, and expression quantitative trait loci (eQTL) analysis was also performed, which are detailed in the supplementary material. scRNA-seq datasets were processed and analyzed using the Seurat (version 4.0.1) package. Trajectory analyses were performed using the Monocle (version 2.18.0) package.

Protein quantification of IL33

IL33 was measured using western blot and immunohistochemistry which is outlined in the supplementary materials.

Statistical Analysis

Wilcoxon signed-rank test was used to statistically analyze paired samples from longitudinal study, while Mann-Whitney nonparametric test was used for unpaired samples from the cross-sectional studies. Bonferroni method was used to correct for multiple testing, and the adjusted p-value less than 0.05 was considered significant for all gene expression results. For one-way anovas Dunnett correction for multiple testing was conducted. Correlation analyses incorporated the non-parametric Spearman correlation test.

Results

***IL-33* gene expression increases following smoking cessation and is overall lower in current smokers compared to ex- and never-smokers**

We investigated the association of smoking with the gene expression of *IL-33* and its receptors, *IL1RL1* and *IL1RAP* in one longitudinal and four cross-sectional studies. Initially, *IL-33*, *IL1RL1* and *IL1RAP* gene expression was quantified in the STOP study where bronchial biopsies of COPD patients and healthy controls were collected before and 12 months after smoking cessation (n=16). *IL-33* gene expression significantly increased after smoking cessation (p=0.003, Figure 2A) regardless of disease status, and a similar but non-significant trend was found for *IL1RL1* (p=0.057, Figure 2B), while no difference was observed for *IL1RAP* (p=0.261, Figure S1A). In four independent cross-sectional studies of bronchial biopsies (Figure 2C-F) and brushes we replicate these findings showing significantly higher *IL-33* gene expression in ex/never- versus current smokers (p<0.05). A trend or significant lower levels in current smokers were observed in these studies for *IL1RL1* (Figure 2G-J), while results were inconsistent for *IL1RAP* (Figure S1A-E). Similar results were found in a microarray dataset of small airways, showing the association between the gene expression of *IL33* and smoking status extends to small airways, where disease-driving pathology in COPD develops (Figure S2) (33).

In addition, we investigated whether acute smoke exposure shows similar effect on the gene expression profile of *IL33*. To this end assessed two additional studies: 1) a longitudinal dataset of bronchial brushings collected before and 24 hours after smoking 3 cigarettes in party smokers who refrained from smoking for at least two days before the baseline visit (TIP study, n=63); and 2) a differentiated *in-vitro* model of primary bronchial epithelial cells treated with whole cigarette smoke extract (34, 35). In both acute smoke exposure studies, there were no significant changes in *IL-33* gene expression in response to smoking (Figure S3A-B).

Influence of genetics on *IL-33* gene expression

To investigate whether an association between genetics and *IL-33* gene expression exists, we performed an expression quantitative trait loci (eQTL) analysis (36). This analysis can assess whether a genetic variant or single nucleotide polymorphism (SNP) has any interaction with nearby or distantly located genes, in this case *IL-33*. We focused on one of the top asthma-SNPs (rs992969) previously shown to influence *IL-33* gene expression (37-41). We performed eQTL in the CRUKPAP study, excluding the never smokers due to small sample size (n=8). Although there was no significant interaction with smoking in the eQTL analysis, we found that the GG and AG variants in the rs992969 SNP had significantly lower *IL-33* gene expression in current smokers compared to ex-smokers (Figure S3C). However, there was no difference between current- and ex-smokers that carried the AA allele. Overall, our results suggest that although the rs992969 SNP is associated with *IL-33* gene expression in the airway, smoking status potentially have a more substantial effect on this relationship.

Splicing variants of *IL1RL1* are not influenced by smoking

There are two main splice variants of IL1RL1 a full length membrane bound variant and a truncated soluble variant that acts as a decoy receptor (42). This analysis was performed to assess whether the decoy receptor is expressed instead of the membrane bound variant, which would indicate a false positive. In two studies where the raw RNA-seq data was available, the expression of these two variants were investigated separately. We found that the membrane to IL1RL1 (soluble and membrane common region) was not significantly different in current smokers compared to ex- or never smokers (Figure S4A&D). Furthermore, both the membrane bound and IL1RL1 (soluble and membrane common region) had similar expression profiles between current and ex/never smokers, indicating that these variants are likely co-expressed (Figure S4B-C&E-F). Thus, it indicates that the splicing does not play a role in the association between the gene expression of IL1RL1 and smoking status.

Association between IL33 activation pathway and smoking

To explore the potential association between the IL-33 pathway and smoking, we used a gene signature derived from multiple cell types (human basophils, type 2 innate lymphoid cells (ILC2), regulatory T cells (Treg) and endothelial cells) treated with IL-33 in vitro(43). This IL-33 activation pathway signature was investigated in the same bulk RNA-sequencing studies. Similar to the gene expression, IL33 activation pathway signature was either significantly lower in current smokers compared to ex/never smokers or upregulated after smoking cessation (Figure 3A-E). Together this analysis showed consistent lower activation of the IL-33 signaling pathway in current-smokers compared to never- and ex-smokers regardless of the disease status, which is likely associated with lower IL-33 levels in the airways.

Protein levels of IL33 is lower in current smokers

Next, we investigated protein levels of IL33 in lung homogenates of current and ex-smoking COPD patients. Western blot staining identified three bands (31 kDa, 20 kDa and 16 kDa) that correspond to known sizes of IL33 protein (Figure 3F). Here we observed that the 31 kDa corresponding to the full-length protein was significantly lower in current smokers compared to ex-smokers matching the transcriptomic results ($p < 0.05$, Figure 3G). Trends for lower levels in current smokers were observed for the 20kDa band (Figure 3H), likely associated with processed active form of IL33 and the 16kDa band corresponding to the smaller IL33 splice variant (NP_001186570.1) (Figure 3I) (44).

High gene expression of *IL-33* in basal cells

Next, we investigated *IL-33* and *IL1RL1* gene expression in major cell types from scRNA-seq data of the Human Lung Cell Atlas. The UMAP and violin plot show that the majority of *IL-33* expressing cells are resting basal cells and endothelial cells (Figure 4A, Figure S5A). While *IL1RL1* was found to be expressed mainly in mast cells, mirroring previous report (45), it was also present in the endothelial aerocyte capillary cells (Figure 4B, Figure S5B). While *IL1RAP* was mainly in monocytes (Figure S5C). Based on the finding, we conducted cellular deconvolution to examine the association between smoking status and cellular composition. This method can be performed in the four bulk RNA-sequencing datasets. Interestingly, the basal cell significantly either increased in smokers after smoking cessation or were lower in proportion in current smokers compared to ex/never smokers (Figure 4C-F). A significant positive correlation between basal cell proportions and *IL33* gene expression was found for all four studies (Figure 4G-J).

***IL-33* gene expression is decreased in smokers potentially due to phenotypic changes in basal cells**

It should be noted that cell deconvolution results are prediction, not a precise representation of cell distribution *in-vivo*. scRNA-seq analyses are deemed more robust than cellular deconvolution of bulk RNA-seq data. They represent variations at the individual cell level, which may be overlooked by bulk analyses. Therefore, to verify the predicted relationship between lower *IL-33* gene expression and lower (predicted) basal cells in smokers, we directly analyzed a single-cell sequencing dataset of airway brushes from healthy smokers (n=6) and never-smokers (n=6) (26). The single-cell mapping shows that in current smokers *IL-33* predominantly expressed in resting basal cells, followed by club/goblet and suprabasal cells (Figure 5A-D). Together these results indicate that *IL-33* gene expression may be specific to a subtype of basal cells. In resting basal, the percentage of cells is significantly lower in current smokers compared to never smokers (Figure 5E). If we solely focus on resting basal cells, we observe a downward trend in the *IL-33* gene expression between smokers and never smokers (p=0.13, Figure 5F).

To validate the findings that current smoking is associated with lower levels of IL33 positive basal cells (resting basal cells) we conducted a double staining for the general basal cell marker p40 and IL33 in lung tissue derived from current and ex/never smokers and calculated the proportion of IL-33 positive cells within the p40 positive basal cells in the airways (Figure 5G-L). We found significantly lower proportion of IL-33 positive p40 cells in non-COPD current smokers compared to COPD ex-smokers and non-COPD never/ex-smokers (FDR<0.05, Figure 5K). In a secondary cohort of current and ex-smoking COPD patients and ex-smoking controls we found no significant difference between the groups, though a similar pattern was observed with lower proportion in COPD current smokers (Figure 5L).

***IL-33* gene expression is decreased during basal cell differentiation**

Since prior findings demonstrated that *IL-33* expression varies between specific basal cell subtypes (46), we next investigated the gene expression of *IL-33* upon differentiation of basal cells. For this we used scRNA-seq data of airway epithelial cell cultures differentiated in air-liquid interface (ALI). These ALI cell culture data offer a more controlled system during which basal cells differentiate into secretory (goblet and club) cells, ciliated cells, and other less abundant luminal cell types. This allows for the distinction between basal cell subtypes (resting basal and suprabasal cells), which may be more abundant in ALI-cultured epithelial cells than in biopsies/brushings (47). To this effect, we analyzed two scRNA-seq datasets; the first study was primary bronchial epithelial cells collected from healthy (n=3) and COPD (n=4, Figure 6A-B), and the second study was primary small airway collected from current (n=3) and never smokers (n=3, Figure 6C-D). Both studies were differentiated in ALI, where the latter study was exposed to cigarette smoke for short-term (4 days) and long-term (28 days). From the violin plots (Figure 6E-F) and the trajectory analysis (Figure 6G-J), we can observe that *IL-33* gene expression was predominantly observed in resting and cycling basal cells, with a rapid decrease in gene expression as these cells transition into suprabasal cells. Together, these analyses show that *IL-33* gene expression is specific to resting and cycling subsets of basal cells.

Smoke exposure is associated with a decrease in resting basal cells and an overall reduction in *IL-33* gene expression *in-vitro* and *in-vivo*

Finally, we investigated the influence of smoke exposure on the latter scRNA-seq study where ALI-differentiated small airways epithelium was exposed to cigarette smoke for 4 days and 28 days. The percentage of resting basal cells decreased significantly in both time periods, as suprabasal cells increased significantly on day 28 of exposure ($p < 0.05$, Figure 6K-L). We also found the *IL-33* gene expression was significantly less in resting basal cells at 4 days after

smoke exposure (Figure 6M-N). These results provide strong evidence that cigarette smoke leads to overall reduction in IL33 expression in both transcriptomic and protein level and that may be due to the decrease in resting basal cells. An overview of all results is present in Figure S6.

Discussion

This study demonstrates that *IL-33* gene expression is lower in the airways of current smokers compared to never/ex-smokers and increases upon smoking cessation, which is supported by the protein data. We further show that *IL-33* is predominantly expressed in resting basal epithelial cells, which occur in lower proportions compared to more differentiated airway epithelial cell types in the airways of current smokers. We provide evidence that the lower gene expression of *IL-33* in current smokers can largely be attributed to a reduction in basal cell proportion, perhaps due to increased differentiation towards squamous and goblet cell subtypes. This is further supported by the protein analysis, where we confirmed lower proportion of IL-33 positive basal cells in current smokers and total IL-33 protein levels were decreased in current smokers. In current smokers, our findings suggest that a distinct inflammatory phenotype is present that is not IL-33 driven. Together, these results may help explain the recent clinical observation that anti-IL-33 treatment is more efficacious in ex-smoking COPD patients than current-smoking.

We show that *IL-33* gene expression and protein levels are lower with current smoking and increases following smoking cessation. We did not find an acute effect of smoking on *IL-33* gene expression in epithelial cells collected by bronchial brushings 24 hours later, suggesting that the effects of smoking only occur with chronic exposure. Our western blot protein findings are in line with prior *in-vivo* human data, showing lower IL-33 protein levels in nasal and

broncho-alveolar lavage in current- versus ex-smokers (11, 12). However, these previous protein studies need to be viewed with caution as Pace *et al.* (12) employed the R&D systems ELISA assay, which was recently highlighted to lack specificity and sensitivity in detecting IL-33 (48), while the immunoassay method by Gómez *et al.* (11) has not been subjected to validation tests. This lack of specificity of IL-33 antibodies is not as much an issue with western blot as we are able to focus on bands that correspond to known sizes of IL33 variants. In contrast, *in-vitro* studies on human bronchial epithelial cell cultures (HBEs) and murine cells found *IL-33* gene expression to increase after whole cigarette smoke exposure for 24 hours and for three separate 1-hr periods per day for four consecutive days, respectively (13, 14). A possible cause for this discrepancy is that, in a closed *in-vitro* system, cells are exposed to cigarette smoke in an acute setting and before or after cell differentiation. Hence, pro-inflammatory responses such as the release of IL-33 may take place before the shifting of cell types occurs.

Recently, anti-IL1RL1, astegolimab, was used to treat asthma and COPD in separate and independent trials. The trials showed that anti-IL1RL1 reduced the asthma exacerbations rate in asthma participants (49), however, in COPD, it did not significantly reduce exacerbations compared to placebo (50). This indicates that targeting just IL1RL1 receptor is insufficient and that IL33 may have additional targets in the body.

We show that changes in *IL-33* gene expression may be related to changes in airway epithelial cell composition. IL-33 was found to be predominantly expressed in resting basal cells, corresponding with previous studies at both transcriptional and protein levels (46, 51, 52). A previous study by Byers *et al.* on airways of COPD patients found through histology that IL-33 is localized to a subset of basal epithelial cells, while being absent in more differentiated

ciliated and secretory epithelial cell types. This matches with the histology done in the current paper. Additionally, IL-33 partially overlapped with the conventional basal cell biomarkers KRT5 and TP63, indicating it is not expressed in all basal epithelial cells but likely only in a distinct proportion (46). This finding is supported by our single-cell analyses of differentiated airway epithelial cells grown where we particularly found *IL-33* gene expression in resting and cycling basal cells, further suggesting that the lower levels of *IL-33* gene expression in current smokers is to a large extent explained by a reduction in a specific basal cell subtype (46).

We were able to show that resting basal cells decrease during smoke exposure *in-vivo* and *in-vitro*. A recent meta-analysis of lung single-cell data found an overall reduction of basal cells in current smokers compared to non-smokers supporting these findings (53). Of interest histological staining of KRT5 a basal cell marker in a previous study showed a trend towards a decrease in absolute numbers of basal cells in current smokers versus never smokers (26). A lower number of basal cells may result from either cell death of basal cells in response to inflammation or from their transition into different cell types in association with their progenitor role (54, 55). Based on our trajectory analyses and current literature (46), the latter is the more plausible.

Endothelial cells were also found to have high levels of *IL-33*; however, they comprise a very small cell proportion of the bronchial biopsy samples. Despite this, they may still play an important role in the release of IL-33, especially into the bloodstream.

During smoking cessation, we observed an increase of the basal cell population returning the reservoir of *IL-33* in the airways. However, return of this *IL-33* reservoir paired together with the emphysema and cellular death associated with COPD, which continues after smoking

cessation, results in the release of this trapped *IL-33*, likely leads to *IL-33* driven inflammation, which would be absent from asymptomatic ex-smokers due to the lack of continued cellular damage. Interestingly our *IL-33* pathway findings suggest there is a shift of the main inflammation profiles following smoking cessation in COPD from smoking-induced oxidative stress to a more *IL-33*-driven inflammation. This finding may lead to a paradigm shift in our understanding of COPD pathology; however, further studies need to be conducted to validate this theory.

There are several limitations to our study. First, the *in-vivo* single-cell data analyzed in our current study consists of healthy individuals. Future bronchial epithelial data from the human cell atlas should include subjects with different lung diseases as the presence of the disease may greatly affect cellular activity and phenotypes. It is also important for further studies to investigate the mechanisms of regulation and effects of *IL-33* using single-cell data in a longitudinal setting.

In conclusion, we show that *IL-33* expression at both gene and protein level are lower in current-smokers than in ex-smokers. Lower expression of *IL-33* is likely due to the differentiation of resting basal cells towards a more differentiated subtype (i.e., suprabasal) as *IL-33* is predominantly expressed in the least differentiated epithelial cells. Our findings help explain the clinical observation of the greater efficacy of a recent antibody-based anti-*IL-33* treatment in ex-smokers compared to current smokers with COPD as *IL-33* expression appears to be inherently lower in current smokers.

References

1. Celli BR, Wedzicha JA. Update on clinical aspects of chronic obstructive pulmonary disease. *New England Journal of Medicine* 2019; 381: 1257-1266.
2. Barnes PJ, Burney PG, Silverman EK, Celli BR, Vestbo J, Wedzicha JA, Wouters EF. Chronic obstructive pulmonary disease. *Nat Rev Dis Primers* 2015; 1: 15076.
3. Zhao J, Zhao Y. Interleukin-33 and its Receptor in Pulmonary Inflammatory Diseases. *Crit Rev Immunol* 2015; 35: 451-461.
4. Le H, Kim W, Kim J, Cho HR, Kwon B. Interleukin-33: a mediator of inflammation targeting hematopoietic stem and progenitor cells and their progenies. *Front Immunol* 2013; 4: 104.
5. Schmitz J, Owyang A, Oldham E, Song Y, Murphy E, McClanahan TK, Zurawski G, Moshrefi M, Qin J, Li X, Gorman DM, Bazan JF, Kastelein RA. IL-33, an Interleukin-1-like Cytokine that Signals via the IL-1 Receptor-Related Protein ST2 and Induces T Helper Type 2-Associated Cytokines. *Immunity* 2005; 23: 479-490.
6. Liew FY. Cigarette smoke resets the Alarmin IL-33 in COPD. *Immunity* 2015; 42: 401-403.
7. Gabryelska A, Kuna P, Antczak A, Białasiewicz P, Panek M. IL-33 Mediated Inflammation in Chronic Respiratory Diseases-Understanding the Role of the Member of IL-1 Superfamily. *Front Immunol* 2019; 10: 692.
8. Wechsler ME, Ruddy MK, Pavord ID, Israel E, Rabe KF, Ford LB, Maspero JF, Abdulai RM, Hu C-C, Martincova R. Efficacy and safety of itepekimab in patients with moderate-to-severe asthma. *New England Journal of Medicine* 2021; 385: 1656-1668.
9. Rabe KF, Celli BR, Wechsler ME, Abdulai RM, Luo X, Boomsma MM, Staudinger H, Horowitz JE, Baras A, Ferreira MA. Safety and efficacy of itepekimab in patients with moderate-to-severe COPD: a genetic association study and randomised, double-blind, phase 2a trial. *The Lancet Respiratory Medicine* 2021; 9: 1288-1298.
10. Abonia JP, Blanchard C, Butz BB, Rainey HF, Collins MH, Stringer K, Putnam PE, Rothenberg ME. Involvement of mast cells in eosinophilic esophagitis. *Journal of Allergy and Clinical Immunology* 2010; 126: 140-149.
11. Gómez RM, Croce VH, Zernotti ME, Muiño JC. Active smoking effect in allergic rhinitis. *World Allergy Organization Journal* 2021; 14: 100504.
12. Pace E, Di Sano C, Sciarrino S, Scafidi V, Ferraro M, Chiappara G, Siena L, Gangemi S, Vitulo P, Giarratano A. Cigarette smoke alters IL-33 expression and release in airway epithelial cells. *Biochimica et Biophysica Acta (BBA)-Molecular Basis of Disease* 2014; 1842: 1630-1637.
13. Qiu C, Li Y, Li M, Li M, Liu X, McSharry C, Xu D. Anti-interleukin-33 inhibits cigarette smoke-induced lung inflammation in mice. *Immunology* 2013; 138: 76-82.
14. Xia J, Zhao J, Shang J, Li M, Zeng Z, Zhao J, Wang J, Xu Y, Xie J. Increased IL-33 expression in chronic obstructive pulmonary disease. *American Journal of Physiology-Lung Cellular and Molecular Physiology* 2015; 308: L619-L627.
15. Kearley J, Silver JS, Sanden C, Liu Z, Berlin AA, White N, Mori M, Pham TH, Ward CK, Criner GJ, Marchetti N, Mustelin T, Erjefalt JS, Kolbeck R, Humbles AA. Cigarette smoke silences innate lymphoid cell function and facilitates an exacerbated type I interleukin-33-dependent response to infection. *Immunity* 2015; 42: 566-579.
16. Allinne J, Scott G, Lim WK, Birchard D, Erjefält JS, Sandén C, Ben LH, Agrawal A, Kaur N, Kim JH, Kamat V, Fury W, Huang T, Stahl N, Yancopoulos GD, Murphy AJ, Sleeman MA, Orenco JM. IL-33 blockade affects mediators of persistence and exacerbation in a model of chronic airway inflammation. *J Allergy Clin Immunol* 2019; 144: 1624-1637.e1610.

17. Rabe KF, Celli BR, Wechsler ME, Abdulai R, Luo X, Boomsma MM, Staudinger H, Horowitz JE, Baras A, Ferreira MA, Ruddy MK, Nivens MC, Amin N, Weinreich DM, Yancopoulos GD, Goulaouic H. Efficacy and safety of itepekimab in patients with moderate to severe COPD. *Lancet Respiratory Medicine* 2021.
18. Faiz A, Boedijono F, Timens W, Nawijn M, Hansbro P, Mahbub R, Johansen M, Brandsma C, Heijink I, Massip F. The regulation of IL33 following smoking cessation. *Eur Respiratory Soc*; 2022.
19. Faiz A, Mahbub R, Sabrina Boedijono F, Timens W, Nawijn M, Hansbro P, D. Johansen M, Brandsma C-A, Heijink I, Massip F. Using Single Cell Sequencing to Understand Treatment Response to Anti-IL33 Treatment in Chronic Obstructive Pulmonary Disease (COPD). B107 COPD: FROM OMICS TO TREATMENT: American Thoracic Society; 2023. p. A4414-A4414.
20. Willemse BW, ten Hacken NH, Rutgers B, Lesman-Leegte IG, Postma DS, Timens W. Effect of 1-year smoking cessation on airway inflammation in COPD and asymptomatic smokers. *European Respiratory Journal* 2005; 26: 835-845.
21. Faiz A, Steiling K, Roffel MP, Postma DS, Spira A, Lenburg ME, Borggrewe M, Eijgenraam TR, Jonker MR, Koppelman GH. Effect of long-term corticosteroid treatment on microRNA and gene-expression profiles in COPD. *European Respiratory Journal* 2019; 53.
22. van den Berge M, Steiling K, Timens W, Hiemstra PS, Sterk PJ, Heijink IH, Liu G, Alekseyev YO, Lenburg ME, Spira A, Postma DS. Airway gene expression in COPD is dynamic with inhaled corticosteroid treatment and reflects biological pathways associated with disease activity. *Thorax* 2014; 69: 14-23.
23. Steiling K, Van Den Berge M, Hijazi K, Florido R, Campbell J, Liu G, Xiao J, Zhang X, Duclos G, Drizik E. A dynamic bronchial airway gene expression signature of chronic obstructive pulmonary disease and lung function impairment. *American journal of respiratory and critical care medicine* 2013; 187: 933-942.
24. Vermeulen CJ, Xu C-J, Vonk JM, Ten Hacken NH, Timens W, Heijink IH, Nawijn MC, Boekhoudt J, van Oosterhout AJ, Affleck K. Differential DNA methylation in bronchial biopsies between persistent asthma and asthma in remission. *European Respiratory Journal* 2020; 55.
25. Aliee H, Massip F, Qi C, Stella de Biase M, van Nijnatten JL, Kersten ETG, Kermani NZ, Khuder B, Vonk JM, Vermeulen RCH, Neighbors M, Tew GW, Grimbaldston M, Ten Hacken NHT, Hu S, Guo Y, Zhang X, Sun K, Hiemstra PS, Ponder BA, Makela MJ, Malmstrom K, Rintoul RC, Reyfman PA, Theis FJ, Brandsma C-A, Adcock I, Timens W, Xu CJ, van den Berge M, Schwarz RF, Koppelman GH, Nawijn MC, Faiz A. Determinants of SARS-CoV-2 receptor gene expression in upper and lower airways. *medRxiv* 2020: 2020.2008.2031.20169946.
26. Duclos GE, Teixeira VH, Autissier P, Gesthalter YB, Reinders-Luinge MA, Terrano R, Dumas YM, Liu G, Mazzilli SA, Brandsma C-A, van den Berge M, Janes SM, Timens W, Lenburg ME, Spira A, Campbell JD, Beane J. Characterizing smoking-induced transcriptional heterogeneity in the human bronchial epithelium at single-cell resolution. *Science Advances* 2019; 5: eaaw3413.
27. Johansen MD, Mahbub RM, Idrees S, Nguyen DH, Miemczyk S, Pathinayake P, Nichol K, Hansbro NG, Gearing LJ, Hertzog PJ, Gallego-Ortega D, Britton WJ, Saunders BM, Wark PA, Faiz A, Hansbro PM. Increased SARS-CoV-2 Infection, Protease, and Inflammatory Responses in Chronic Obstructive Pulmonary Disease Primary Bronchial Epithelial Cells Defined with Single-Cell RNA Sequencing. *Am J Respir Crit Care Med* 2022; 206: 712-729.

28. Wohnhaas CT, Gindele JA, Kiechle T, Shen Y, Leparo GG, Stierstorfer B, Stahl H, Gantner F, Viollet C, Schymeinsky J, Baum P. Cigarette Smoke Specifically Affects Small Airway Epithelial Cell Populations and Triggers the Expansion of Inflammatory and Squamous Differentiation Associated Basal Cells. *Int J Mol Sci* 2021; 22.
29. McCarthy DJ, Chen Y, Smyth GK. Differential expression analysis of multifactor RNA-Seq experiments with respect to biological variation. *Nucleic Acids Research* 2012; 40: 4288-4297.
30. Robinson MD, McCarthy DJ, Smyth GK. edgeR: a Bioconductor package for differential expression analysis of digital gene expression data. *Bioinformatics* 2009; 26: 139-140.
31. Ritchie ME, Phipson B, Wu D, Hu Y, Law CW, Shi W, Smyth GK. limma powers differential expression analyses for RNA-sequencing and microarray studies. *Nucleic Acids Research* 2015; 43: e47-e47.
32. Duclos GE, Teixeira VH, Autissier P, Gesthalter YB, Reinders-Luinge MA, Terrano R, Dumas YM, Liu G, Mazzilli SA, Brandsma C-A. Characterizing smoking-induced transcriptional heterogeneity in the human bronchial epithelium at single-cell resolution. *Science Advances* 2019; 5: eaaw3413.
33. Ammous Z, Hackett NR, Butler MW, Raman T, Dolgalev I, O'Connor TP, Harvey B-G, Crystal RG. Variability in Small Airway Epithelial Gene Expression Among Normal Smokers. *Chest* 2008; 133: 1344-1353.
34. Billatos E, Faiz A, Gesthalter Y, LeClerc A, Alekseyev Y, Xiao X, Liu G, ten Hacken NH, Heijink I, Timens W. Impact of acute exposure to cigarette smoke on airway gene expression. *Physiological genomics* 2018; 50: 705-713.
35. van der Does AM, Mahbub RM, Ninaber DK, Rathnayake SNH, Timens W, van den Berge M, Aliee H, Theis FJ, Nawijn MC, Hiemstra PS, Faiz A. Early transcriptional responses of bronchial epithelial cells to whole cigarette smoke mirror those of in-vivo exposed human bronchial mucosa. *Respir Res* 2022; 23: 227.
36. Shabalina AA. Matrix eQTL: Ultra fast eQTL analysis via large matrix operations. *Bioinformatics* 2012; 28: 1353-1358.
37. Aneas I, Decker DC, Howard CL, Sobreira DR, Sakabe NJ, Blaine KM, Stein MM, Hrusch CL, Montefiori LE, Tena J, Magnaye KM, Clay SM, Gern JE, Jackson DJ, Altman MC, Naureckas ET, Hogarth DK, White SR, Gomez-Skarmeta JL, Schoetler N, Ober C, Sperling AI, Nobrega MA. Asthma-associated variants induce *IL33* differential expression through a novel regulatory region. *bioRxiv* 2020: 2020.2009.2009.290098.
38. Grotenboer NS, Ketelaar ME, Koppelman GH, Nawijn MC. Decoding asthma: translating genetic variation in *IL33* and *IL1RL1* into disease pathophysiology. *Journal of allergy and clinical immunology* 2013; 131: 856-865. e859.
39. Imkamp K, Berg M, Vermeulen C, Heijink I, Guryev V, Koppelman G, van den Berge M, Faiz A, Kerstjens H. Comparison of gene expression profiles from nasal and bronchial brushes. *European Respiratory Journal* 2017; 50: OA2910.
40. Ketelaar ME, Portelli MA, Dijk FN, Shrine N, Faiz A, Vermeulen CJ, Xu CJ, Hankinson J, Bhaker S, Henry AP. Phenotypic and functional translation of *IL33* genetics in asthma. *Journal of Allergy and Clinical Immunology* 2021; 147: 144-157.
41. Li X, Hastie AT, Hawkins GA, Moore WC, Ampleford EJ, Milosevic J, Li H, Busse WW, Erzurum SC, Kaminski N, Wenzel SE, Meyers DA, Bleeker ER. eQTL of bronchial epithelial cells and bronchial alveolar lavage deciphers GWAS-identified asthma genes. *Allergy* 2015; 70: 1309-1318.

42. Gordon ED, Palandra J, Wesolowska-Andersen A, Ringel L, Rios CL, Lachowicz-Scroggins ME, Sharp LZ, Everman JL, MacLeod HJ, Lee JW. IL1RL1 asthma risk variants regulate airway type 2 inflammation. *JCI insight* 2016; 1.
43. Badi YE, Salcman B, Taylor A, Rana B, Kermani NZ, Riley JH, Worsley S, Mumby S, Dahlen SE, Cousins D. IL1RAP expression and the enrichment of IL-33 activation signatures in severe neutrophilic asthma. *Allergy* 2023; 78: 156-167.
44. Talabot-Ayer D, Lamacchia C, Gabay C, Palmer G. Interleukin-33 is biologically active independently of caspase-1 cleavage. *Journal of Biological Chemistry* 2009; 284: 19420-19426.
45. Faiz A, Pavlidis S, Kuo C, Rowe A, Hiemstra P, Timens W, Berg M, Wisman M, Guo Y, Djukanovic R. Novel Type 2-high gene clusters associated with corticosteroid sensitivity in COPD. *BioRxiv* 2020.
46. Byers DE, Alexander-Brett J, Patel AC, Agapov E, Dang-Vu G, Jin X, Wu K, You Y, Alevy Y, Girard J-P, Stappenbeck TS, Patterson GA, Pierce RA, Brody SL, Holtzman MJ. Long-term IL-33-producing epithelial progenitor cells in chronic obstructive lung disease. *The Journal of Clinical Investigation* 2013; 123: 3967-3982.
47. Dvorak A, Tilley AE, Shaykhiev R, Wang R, Crystal RG. Do airway epithelium air-liquid cultures represent the in vivo airway epithelium transcriptome? *American journal of respiratory cell and molecular biology* 2011; 44: 465-473.
48. Ketelaar ME, Nawijn MC, Shaw DE, Koppelman GH, Sayers I. The challenge of measuring IL-33 in serum using commercial ELISA: lessons from asthma. *Clinical & Experimental Allergy* 2016; 46: 884-887.
49. Kelsen SG, Agache IO, Soong W, Israel E, Chupp GL, Cheung DS, Theess W, Yang X, Staton TL, Choy DF. Astegolimab (anti-ST2) efficacy and safety in adults with severe asthma: A randomized clinical trial. *Journal of allergy and clinical immunology* 2021; 148: 790-798.
50. Yousuf AJ, Mohammed S, Carr L, Ramsheh MY, Micieli C, Mistry V, Haldar K, Wright A, Novotny P, Parker S. Astegolimab, an anti-ST2, in chronic obstructive pulmonary disease (COPD-ST2OP): a phase 2a, placebo-controlled trial. *The Lancet Respiratory Medicine* 2022; 10: 469-477.
51. Goldfarbmuren KC, Jackson ND, Sajuthi SP, Dyjack N, Li KS, Rios CL, Plender EG, Montgomery MT, Everman JL, Bratcher PE. Dissecting the cellular specificity of smoking effects and reconstructing lineages in the human airway epithelium. *Nature communications* 2020; 11: 1-21.
52. Osei ET, Mostaço-Guidolin LB, Hsieh A, Warner SM, May A-F, Wang M, Cole DJ, Maksym GN, Hallstrand TS, Timens W. Epithelial-interleukin-1 inhibits collagen formation by airway fibroblasts: Implications for asthma. *Scientific reports* 2020; 10: 1-14.
53. Nakayama J, Yamamoto Y. Single-cell meta-analysis of cigarette smoking lung atlas. *bioRxiv* 2021.
54. Hong KU, Reynolds SD, Watkins S, Fuchs E, Stripp BR. Basal Cells Are a Multipotent Progenitor Capable of Renewing the Bronchial Epithelium. *The American Journal of Pathology* 2004; 164: 577-588.
55. Rock JR, Onaitis MW, Rawlins EL, Lu Y, Clark CP, Xue Y, Randell SH, Hogan BLM. Basal cells as stem cells of the mouse trachea and human airway epithelium. *Proceedings of the National Academy of Sciences* 2009; 106: 12771-12775.

Table 1: Baseline characteristics of the datasets

Study	Sample Types	Smoking Status	n (%)	Mean Age (SD)	Gender male n(%)	Mean Pack years (SD)	Mean FEV1 % (SD) Prediction	Mean FEV1/FVC (SD)	Platform	Profiling Assay
Bulk RNA-sequencing/microarray studies										
STOP smoking RNA-seq (Longitudinal) (20)	Bronchial Biopsies	Current smokers	16 (100)	54 (6.6)	9 (56.3)	32.3 (13.7)	82.1 (23.3)	70.6 (14.3)	Bulk RNA-Seq	Illumina HiSeq 2500
GLUCOLD Microarray and RNA-seq (21, 22)	Bronchial Biopsies	Current smokers	36 (62.1)	57.8 (7.4)	28 (77.8)	45 (15.3)	56.5 (10.4)	50.7 (9)	Microarray & Bulk RNA Seq	Affymetrix HG 1.0 ST microArray & Illumina HiSeq 2500
		Ex-smokers	22 (37.9)	63.3 (8.18)	20 (90.9)	44.48 (27.8)	54.6 (9.5)	46.8 (8.5)		
COPD Microarray (GSE37147) (23)	Bronchial Brushings	Current smokers	30 (34.5)	63.2 (6.68)	16 (53.3)	47.5 (13.6)	57.6 (16.4)	56.9 (11.7)	Microarray	Affymetrix HG 1.0 ST microArray
		Ex-smokers	57 (65.5)	66.1 (5.6)	36 (63.2)	52.9 (28.1)	61.6 (12.1)	60.3 (7.5)		
NORM RNA-seq (24)	Bronchial Biopsies and Brushings	Current smokers	37 (48.1)	41.6 (15.2)	22 (59.5)	18.8 (15.1)	99.3 (9.2)	78.2 (6.1)	Bulk RNA Seq	Illumina HiSeq 2500
		Non-Smokers	40 (51.9)	38.5 (18.9)	20 (50)	0 (0)	101.5 (11.9)	80.7 (6.8)		
CRUKPAP RNA-seq (25)	Bronchial brushings	Current smokers	77 (32.6)	63.3 (10.9)	49 (63.6)	44.3 (20.8)	N/A	N/A	Bulk RNA-seq	Illumina HiSeq 2500
		Ex-smokers	151 (64)	69.3 (9.1)	104 (68.9)	41.3 (27.3)	N/A	N/A		

		Never-smokers	8 (3.4)	66.9 (8.5)	5 (62.5)	0 (0)	N/A	N/A		
Single-cell RNA-sequencing studies										
Smokers <i>in-vivo</i> scRNA-seq (GSE131391) (32)	Bronchial brushings	Current smokers	6 (50)	42.7 (9.7)	3 (50)	15.3 (7.9)	N/A	82.7 (5.5)	Single cell RNA seq	Illumina HiSeq 2500
		Never-smokers	6 (50)	29.5 (7.6)	3 (50)	0 (0)	N/A	82.6 (3.7)		
COPD ALI <i>in-vitro</i> scRNA-seq (27)	Primary bronchial airway epithelial cells from healthy never-smokers and COPD ex/current smokers	Current smokers	2 (28.6)	72.5 (7.8)	2 (66.7)	55(4.2)	66.5 (7.8)	15.5 (4.9)	Single Cell RNA-Seq	BD Rhapsody Express Cell Capture System
		Ex-smokers	2 (28.6)	80.5 (6.4)	0 (0)	62 (12.7)	60.5 (9.2)	12.5 (12.0)		
		Never-smokers	3 (42.6)	69 (12.2)	1 (33.3)	0 (0)	90 (18.3)	74.3 (5.1)		
Smoke ALI CS <i>in-vitro</i> scRNA-seq (28)	Primary small airway epithelial cells from healthy never-smokers and COPD donors	Current smokers	3 (50)	56.7 (5.5)	0 (0)	N/A	N/A	N/A	Single Cell RNA-Seq	Cell Ranger v2.1.1 (10x Genomics, Pleasanton, CA, USA)
		Never smokers	3 (50)	49 (15.7)	1 (33.3)	N/A	N/A	N/A		

Figure Legends

Figure 1. Method flowchart of the current study. One longitudinal and four cross-sectional in-vivo studies were analyzed to assess the gene expression profile of *IL-33* and *IL-33* pathway related genes. Cellular deconvolution was performed on the studies where bulk RNA-sequencing was performed, as the method is not suitable for microarray study. One in-vivo and two in-vitro single-cell RNA-sequencing studies were analyzed to assess the *IL-33* expression at single-cell level and cell trajectory (20-25, 27, 28, 32).

Figure 2. Expression of *IL-33* and *IL1RL1* in bronchial datasets. **A** *IL-33* and **B** *IL1RL1* expression levels from the STOP study of bronchial biopsies (n=16) pre and post 12 months smoking cessation. **C** *IL-33* and **G** *IL1RL1* expression levels of bronchial biopsies from the GLUCOLD study of ex-smokers (n=33) and current smoker (n=46) COPD patients. **D** *IL-33* and **H** *IL1RL1* expression levels of bronchial brushes from the COPD microarray study of ex-smokers (n=57) and current smokers (n=30) COPD patients (GSE37147). **E** *IL-33* and **I** *IL1RL1* expression of bronchial biopsies from the NORM study of never (n=40) and current (n=37) healthy smokers. **F** *IL-33* and **J** *IL1RL1* expression of bronchial biopsies from the CRUKPAP study of never (n=8), ex- (n=151) and current (n=77) smokers. All analyses were corrected for age and gender. The numbers shown are p-values taken from results of differential expression analyses conducted in edgeR, corrected for age and gender. Error bars are representing the standard deviation. P-values shown are FDR corrected for the number of genes tested.

Figure 3. The influence of smoking status on the *IL-33* pathway and protein levels. *IL-33* activation pathway analysis from **A** STOP study of bronchial biopsies (n=16) during current smoking activity and 1 year after cessation; **B** GLUCOLD study of ex-smokers (n=33) and current smoker (n=46) COPD patients; **C** COPD microarray study of bronchial brushings from ex-smokers (n=57) and current smokers (n=30); **D** NORM study of bronchial biopsies from healthy never- (n=40) and current- (n=37) smokers; and **E** CRUKPAP study of bronchial biopsies from never (n=8), ex- (n=151) and current (n=77) smokers. **F** Western blot of whole tissue lysates from COPD current (n=10) and ex-smokers (n=9) for *IL33* and b-actin. Quantification of **G** 31kDa (full length protein) **H** 20 kDa (processed active form) and **I** 16 kDa (small *IL33* isoform) bands corrected by b-actin. P-values were acquired from Wilcoxon signed-rank test for paired analyses and Mann-Whitney for unpaired analyses. Error bars represent the standard deviation.

Figure 4. High expression of *IL-33* in basal cells. **A-B** UMAP of *IL-33* and *IL1RL1* expression of samples taken from the lung and airways Human lung cell atlas V1.0. Predicted basal cell percentages based on cellular deconvolution from **C** STOP study of bronchial biopsy RNA-seq data before and after 1 year of smoking cessation (n=16), **D** GLUCOLD study of bronchial biopsies of ex-smokers (n=33) and current smoker (n=46) COPD patients, **E** NORM study of never- (n=40) and current- (n=37) respiratory healthy smokers, and **F** CRUKPAP study of current- (n=77) and ex- (n=151) and never- (n=8) smokers. P-values of were obtained from the Mann-Whitney nonparametric unpaired t-test. **G** Correlation between change in basal cell percentage and change in *IL-33* expression from STOP study of pre and post smoking cessation. Correlation between basal cells percentage and *IL-33* expression levels in bronchial biopsies from **H** GLUCOLD study of current- (n=46) and ex-smoking (n=33), **I** NORM study of never- (n=40) and current- (n=37) healthy respiratory smokers and **J** CRUKPAP study of

never (n=8), ex- (n=151) and current (n=77) smokers. P-values were obtained from the nonparametric Spearman correlation analysis. Significant result = $p < 0.05$. Error bars represent the standard deviation. Error bars represent the standard deviation.

Figure 5. Expression of *IL-33* in current smokers compared to never smokers in single-cell and protein level. **A** UMAP of cell type clusters of bronchial brushes from never (n=6) and current smokers (n=6) at single-cell RNA-sequencing dataset (GSE131391). UMAP of *IL-33* expression in different cell clusters of **B** never smokers and **C** current smokers. **D** Violin plots of *IL-33* expression across cell types separated based on smoking status. **E** Proportion of resting basal (%) in never-smokers and current smokers. **F** Expression of *IL-33* in resting basal cell population. Mann-Whitney nonparametric unpaired t-test was performed to assess significance. Error bars are representing the standard deviation. Immunofluorescent staining for *IL-33* and p40 were performed in lung tissue sections. A representative image of **G** DAPI. **H** p40 (polyclonal rabbit, anti-human, ab 167612, 1:100), **I** *IL-33* antibody (monoclonal mouse, anti-human, ALX-804-840-C100, 1:800), **J** merged lung tissue section. **K** Staining quantification of the percentage of *IL-33* positive p40+ cells in current smokers (n=9), ex/never smokers (n=26) and ex-smoking COPD patients (n=25). **L** Secondary cohort staining quantification of the percentage of p40+ cells positive for *IL-33* in COPD current smokers (n=9), COPD ex-smokers (n=7) and ex-smoking non-COPD patients (n=7). One-way a nova was conducted with a Dunnett p-value correction for multiple testing. Error bars represent the standard deviation.

Figure 6. Expression of *IL-33* in during basal cell differentiation in single-cell RNA-sequencing *in-vitro* studies. Two *in-vitro* single-cell RNA-sequencing of airway epithelial cells differentiated at air-liquid interface were analyzed. The first was performed on the bronchial epithelial cells collected from healthy never-smokers (n=3) and COPD ex/current smokers (n=4); and the second was performed on small airway epithelial cells collected from healthy never smokers (n=3) and COPD current smokers (n=3). UMAP and the *IL-33* expression of **A-B** the first and **C-D** the second study. Violin plot of the expression of *IL-33* is shown for **E** the first and **F** the second single-cell study. The cell trajectory of different cellular subpopulations along with *IL-33* expression for **G-H** the first and **I-J** the second *in-vitro* study. The arrow represents the direction of the cell trajectory. Percentage of **K** resting basal cell and **L** suprabasal cells from the second single cell study where the airway epithelial cells were exposed to acute (4 days) and chronic (28 days) cigarette smoke. **M** Delta heatmap of the *IL-33* expression in smoke exposure compared to air were shown for different cell-types. The color scale is the change in expression of *IL-33* in smoke exposure compared to air. There are grey blocks in the heatmap which are missing values, as there were missing values in smoke or air for the respective sample. **N** A dot plot representing the *IL-33* expression in resting basal cells for acute (4 days) and chronic (28 days) exposure in the second single cell study.

Conflict of Interest statement

AF, RM, FSB, MJ, SDP, MIT, AvdD, PAW, FM, RFS, MSB, IHH, MN, PSH, MvdB, MH, HK, WT, PH, CB, IMA, KFC have no conflict of interest. HX, HG, RA EdR, DC are employees of Sanofi. MCN, SH, DL are employees of Regeneron.

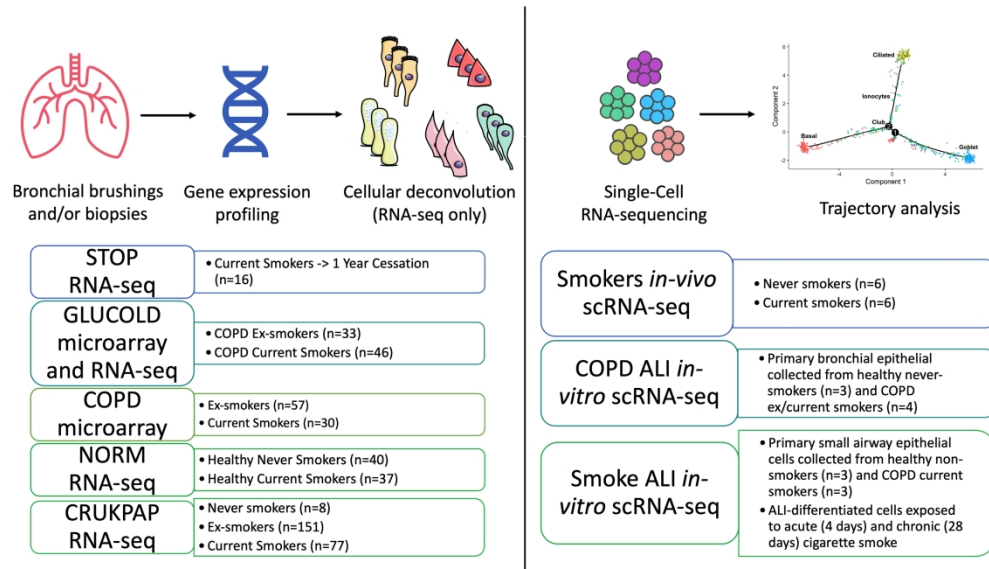


Figure 1. Method flowchart of the current study. One longitudinal and four cross-sectional *in-vivo* studies were analyzed to assess the gene expression profile of IL-33 and IL-33 pathway related genes. Cellular deconvolution was performed on the studies where bulk RNA-sequencing was performed, as the method is not suitable for microarray study. One *in-vivo* and two *in-vitro* single-cell RNA-sequencing studies were analyzed to assess the IL-33 expression at single-cell level and cell trajectory (20-25, 27, 28, 33).

280x160mm (300 x 300 DPI)

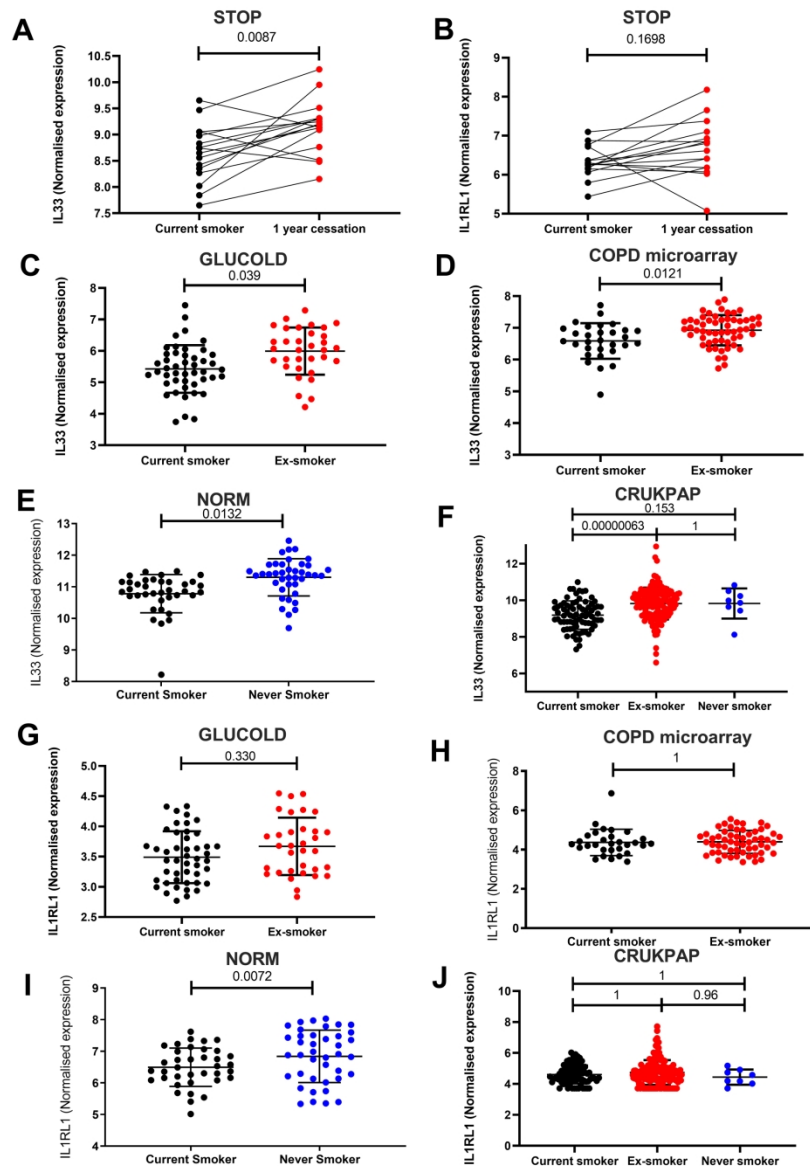


Figure 2.

Expression of IL-33 and IL1RL1 in bronchial datasets. A IL-33 and B IL1RL1 expression levels from the STOP study of bronchial biopsies (n=16) pre and post 12 months smoking cessation. C IL-33 and G IL1RL1 expression levels of bronchial biopsies from the GLUCOLD study of ex-smokers (n=33) and current smoker (n=46) COPD patients. D IL-33 and H IL1RL1 expression levels of bronchial brushes from the COPD microarray study of ex-smokers (n=57) and current smokers (n=30) COPD patients (GSE37147). E IL-33 and I IL1RL1 expression of bronchial biopsies from the NORM study of never (n=40) and current (n=37) healthy smokers. F IL-33 and J IL1RL1 expression of bronchial biopsies from the CRUKPAP study of never (n=8), ex- (n=151) and current (n=77) smokers. All analyses were corrected for age and gender. The numbers shown are p-values taken from results of differential expression analyses conducted in edgeR, corrected for age and gender. Error bars are representing the standard deviation. P-values shown are FDR corrected for the number of genes tested.

206x281mm (300 x 300 DPI)

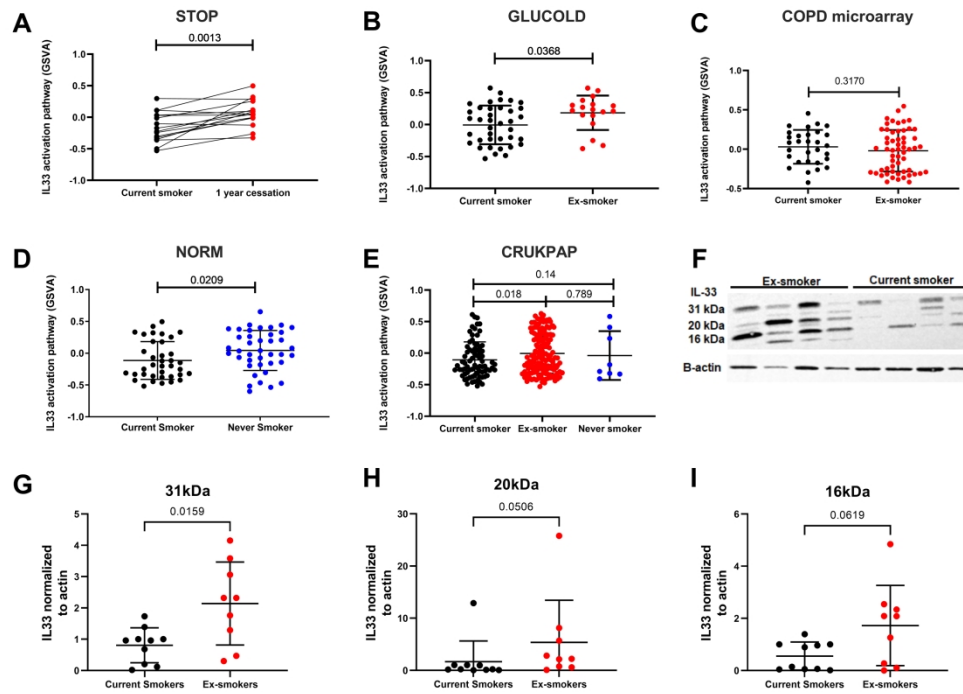


Figure 3. The influence of smoking status on the IL-33 pathway and protein levels. IL-33 activation pathway analysis from A STOP study of bronchial biopsies (n=16) during current smoking activity and 1 year after cessation; B GLUCOLD study of ex-smokers (n=33) and current smoker (n=46) COPD patients; C COPD microarray study of bronchial brushings from ex-smokers (n=57) and current smokers (n=30); D NORM study of bronchial biopsies from healthy never- (n=40) and current- (n=37) smokers; and E CRUKPAP study of bronchial biopsies from never (n=8), ex- (n=151) and current (n=77) smokers. F Western blot of whole tissue lysates from COPD current (n=10) and ex-smokers (n=9) for IL33 and b-actin. Quantification of G 31kDa (full length protein) H 20 kDa (processed active form) and I 16 kDa (small IL33 isoform) bands corrected by b-actin. P-values were acquired from Wilcoxon signed-rank test for paired analyses and Mann-Whitney for unpaired analyses. Error bars represent the standard deviation.

266x191mm (300 x 300 DPI)

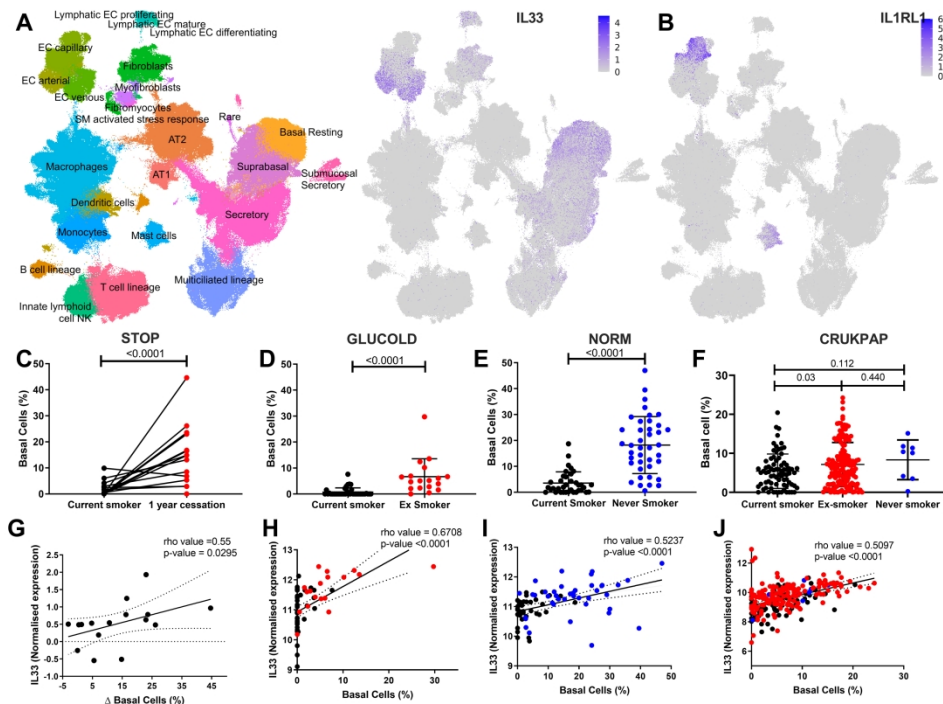


Figure 4. High expression of IL-33 in basal cells. A-B UMAP of IL-33 and IL1RL1 expression of samples taken from the lung and airways Human lung cell atlas V1.0. Predicted basal cell percentages based on cellular deconvolution from C STOP study of bronchial biopsy RNA-seq data before and after 1 year of smoking cessation (n=16), D GLUCOLD study of bronchial biopsies of ex-smokers (n=33) and current smoker (n=46) COPD patients, E NORM study of never- (n=40) and current- (n=37) respiratory healthy smokers, and F CRUKPAP study of current- (n=77) and ex- (n=151) and never- (n=8) smokers. P-values of were obtained from the Mann-Whitney nonparametric unpaired t-test. G Correlation between change in basal cell percentage and change in IL-33 expression from STOP study of pre and post smoking cessation. Correlation between basal cells percentage and IL-33 expression levels in bronchial biopsies from H GLUCOLD study of current- (n=46) and ex-smoking (n=33), I NORM study of never- (n=40) and current- (n=37) healthy respiratory smokers and J CRUKPAP study of never (n=8), ex- (n=151) and current (n=77) smokers. P-values were obtained from the nonparametric Spearman correlation analysis. Significant result = $p < 0.05$. Error bars represent the standard deviation.

294x214mm (300 x 300 DPI)

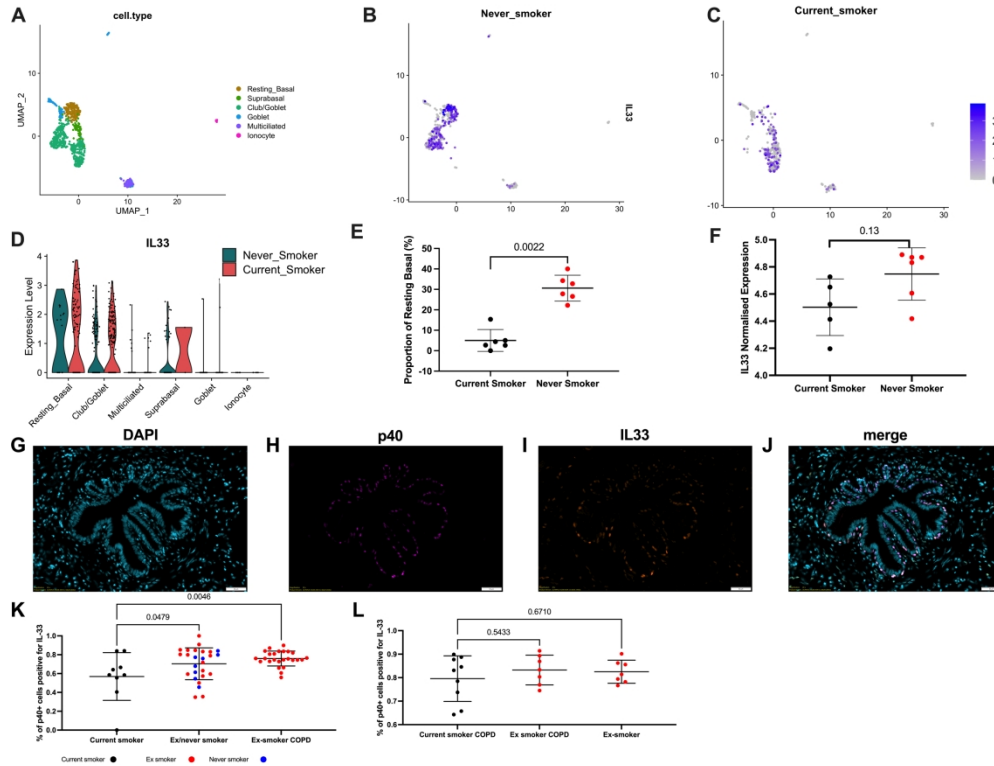


Figure 5. Expression of IL-33 in current smokers compared to never smokers in single-cell and protein level. A UMAP of cell type clusters of bronchial brushes from never (n=6) and current smokers (n=6) at single-cell RNA-sequencing dataset (GSE131391). UMAP of IL-33 expression in different cell clusters of B never smokers and C current smokers. D Violin plots of IL-33 expression across cell types separated based on smoking status. E Proportion of resting basal (%) in never-smokers and current smokers. F Expression of IL-33 in resting basal cell population. Mann-Whitney nonparametric unpaired t-test was performed to assess significance. Error bars are representing the standard deviation. Immunofluorescent staining for IL-33 and p40 were performed in lung tissue sections. A representative image of G DAPI. H p40 (polyclonal rabbit, anti-human, ab 167612, 1:100), I IL-33 antibody (monoclonal mouse, anti-human, ALX-804-840-C100, 1:800), J merged lung tissue section. K Staining quantification of the percentage of IL-33 positive p40+ cells in current smokers (n=9), ex/never smokers (n=26) and ex-smoking COPD patients (n=25). L Secondary cohort staining quantification of the percentage of p40+ cells positive for IL-33 in COPD current smokers (n=9), COPD ex-smokers (n=7) and ex-smoking non-COPD patients (n=7). One-way a nova was conducted with a Dunnett p-value correction for multiple testing. Error bars represent the standard deviation.

279x216mm (300 x 300 DPI)

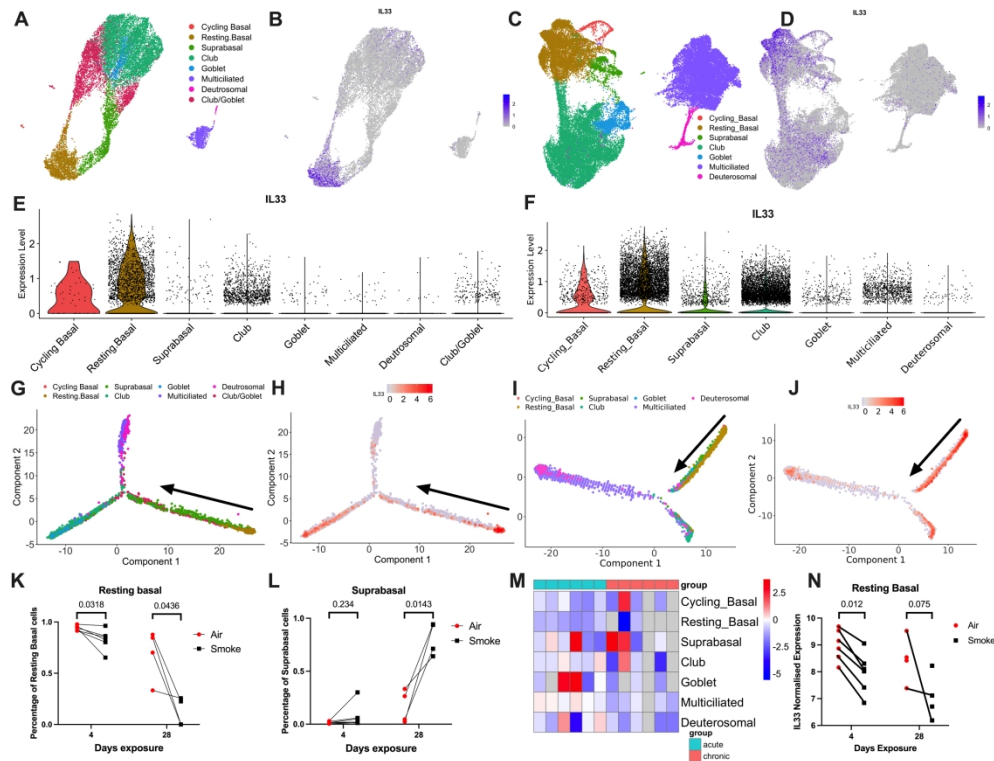


Figure 6. Expression of IL-33 in during basal cell differentiation in single-cell RNA-sequencing in-vitro studies. Two in-vitro single-cell RNA-sequencing of airway epithelial cells differentiated at air-liquid interface were analyzed. The first was performed on the bronchial epithelial cells collected from healthy never-smokers ($n=3$) and COPD ex/current smokers ($n=4$); and the second was performed on small airway epithelial cells collected from healthy never smokers ($n=3$) and COPD current smokers ($n=3$). UMAP and the IL-33 expression of A-B the first and C-D the second study. Violin plot of the expression of IL-33 is shown for E the first and F the second single-cell study. The cell trajectory of different cellular subpopulations along with IL-33 expression for G-H the first and I-J the second in-vitro study. The arrow represents the direction of the cell trajectory. Percentage of K resting basal cell and L suprabasal cells from the second single cell study where the airway epithelial cells were exposed to acute (4 days) and chronic (28 days) cigarette smoke. M Delta heatmap of the IL-33 expression in smoke exposure compared to air were shown for different cell-types. The color scale is the change in expression of IL-33 in smoke exposure compared to air. There are grey blocks in the heatmap which are missing values, as there were missing values in smoke or air for the respective sample. N A dot plot representing the IL-33 expression in resting basal cells for acute (4 days) and chronic (28 days) exposure in the second single cell study.

280x214mm (300 x 300 DPI)

IL-33 expression is lower in current smokers at both transcriptomic and protein level

Alen Faiz, Rashad M. Mahbub, Fia Sabrina Boedijono, Milan I. Tomassen, Wierd Kooistra, Wim Timens, Martijn Nawijn, Philip M. Hansbro, Matt D. Johansen, Simon D. Pouwels, Irene H. Heijink, Florian Massip, Maria Stella de Biase, Roland F. Schwarz, Cambridge Lung Cancer Early Detection Programme, Ian M. Adcock, Kian F. Chung, Anne van der Does, Pieter S. Hiemstra, Helene Goulaouic, Heming Xing, Raolat Abdulai, Emanuele de Rinaldis, Danen Cunoosamy, Sivan Harel, David Lederer, Michael C Nivens, Peter A. Wark, Huib A.M. Kerstjens, Machteld N. Hylkema, Corry-Anke Brandsma, Maarten van den Berge

ONLINE DATA SUPPLEMENT

Additional studies

The TIP study used microarray data to investigate gene expression changes in bronchial brushings of current smokers (n=63) (1). The study collected samples 24 hours after 3 hours of smoking activity and 24 hours after non-smoking activity.

The bulk RNA-sequencing *in-vitro* study used primary bronchial epithelial cells that were isolated from tumour-free resected lung tissue and exposed to whole cigarette smoke or air (2). RNA-sequencing was performed on samples collected at 1h, 4h and 24h after smoke or air exposure.

The COPD small airway were collected from the bronchial brushings of healthy current smokers (n=18), healthy never smokers (n=18) and COPD current smokers (n=18) (3). Samples were then processed using Affymetrix Human Genome U133 Plus 2.0 Array to obtain microarray data. The baseline characteristics for these studies are provided in Table S1.

Single-cell expression profile from Human Lung Cell Atlas

We also looked at the Human Lung Cell Atlas (HCLA) reference which contains scRNA-seq data, integrated from 14 different datasets, and contains approximately 584,000 cells from 107 individuals (29). The gene expression of *IL-33* and its receptors were investigated in this large integrated single-cell data as a reference.

Expression quantitative trait loci (eQTL)

To investigate whether an association between genetics and *IL-33* expression exists, we performed an expression quantitative trait loci (eQTL) analysis (4), focusing on one of the top asthma-SNPs (rs992969) previously shown to influence *IL-33* expression (5-9). This analysis was conducted on the CRUKPAP study, correcting for age and gender.

Cellular deconvolution

Cellular deconvolution of bulk RNA-seq data was performed to estimate the proportions of different cell types from the gene expression for all bulk RNA-Seq datasets. This analysis was performed as previously described (10). Briefly, AutoGeneS software was used to select and filter 400 genes from highly variable ones. The selection was based on minimized correlation and maximized distance between clusters in which genes with the most stable results across cohorts were selected and used to infer major cell type proportions. RNA-seq signatures of club and goblet cells were combined as secretory cells due to their similar gene expression profiles. The RNA-seq data were subsequently normalized to counts per million (CPM), and highly variable (HV) genes (N=5,000) were selected. Bulk deconvolution on all samples was then conducted using the CIBERSORT support vector regression (SVR) method (11). Afterwards, the level of *IL-33* expression was associated with the predicted cell proportions in each dataset. Correlation between cell type and *IL-33* expression was tested using the Spearman correlation test.

Pathway Analysis

An IL-33 activation signature was compared to the RNA-seq datasets (STOP, GLUCOLD, COPD microarray, NORM, CRUKPAP). The IL-33 activation signature was derived from in vitro IL-33-activated human mast cells, basophils, type 2 lymphoid cells and human umbilical vein endothelial cells (HUVEC) (12). Gene set variation analysis (GSVA) was performed for the IL-33 signature using the GSVA package (version 1.38.2) in R (13). The Mann-Whitney test was used to assess statistical significance.

IL1RL1 Splicing

The reads corresponding to common region between the soluble and membrane bound IL1RL1 and the reads unique to only the membrane bound IL1RL1 were investigated separately for two datasets where the Raw RNA-Seq data was available. This method has been previously published for other genes (14).

Immunohistochemical staining

Immunohistochemical staining for IL-33 was performed on paraffin embedded peripheral lung tissue derived from 10 patients. 3 µm thick sections were cut and deparaffinized and rehydrated; followed by antigen retrieval with citrate buffer (10 mM, pH6). Endogenous peroxidase, avidin and biotin were blocked using 0.3% hydrogen peroxidase (H₂O₂) and Avidin/Biotin Blocking Kit (SP-2001, Vector Laboratories, Canada). Blocking was followed by incubation with the primary antibody (monoclonal mouse, anti-human, ALX-804-840-C100, 1:800), diluted in a 1% BSA-PBS, for one hour at room temperature. The sections were washed with PBS and incubated with a biotinylated Rabbit Anti-Mouse (E0413, Dako, Denmark) secondary antibody diluted in 1% human serum + 1% BSA-PBS, after which the sections were washed with PBS and incubated with Horseradish peroxidase (HRP)-conjugated Streptavidin (P0397, Dako, Denmark) diluted in 1% human serum + 1% BSA-PBS. Positive staining was visualized using 15 min incubation with Vector® NovaRED® Substrate (SK-4800, Vector Laboratories, Canada). Sections were counterstained with hematoxylin and scanned at magnification 40x using the Hamamatsu NanoZoomer 2.0HT digital slide scanner (Hamamatsu Photonic K.K., Japan). The R&D anti-IL33 antibody (AF3625) was also used for immunohistology using the protocol previously described (32) at a dilution of 1:400.

Immunofluorescent double staining for IL-33 & p40

Immunohistochemical staining for IL-33 was performed in lung tissues derived from two studies, the first consisted of current smokers (n=9), ex/never smokers (n=26) and ex-smoking COPD patients (n=25) and a second study containing COPD current smokers (n=9), COPD ex-smokers (n=7) and ex-smoking non-COPD patients (n=7). The lung tissues were embedded in paraffin and cut into 3 μ m thick slices. These slices were deparaffinized and rehydrated; followed by antigen retrieval with Tris/HCL buffer (0,1 M, pH = 9). Slides were blocked using 5% BSA/PBS and Avidin/Biotin Blocking Kit (SP-2001, Vector Laboratories, Canada). Blocking was followed by incubation with the primary p40 antibody (polyclonal rabbit, anti-human, ab 167612, 1:100, abcam, UK), diluted in a 1% BSA/PBS, for one hour at room temperature. Secondary antibody incubation for p40 used polyclonal Donkey Anti-Rabbit immunoglobulins (A31573, 1:100, Alexa Fluor™, U.S.A) at room temperature, diluted in 1% human serum + 1% BSA/PBS. Next, slides were incubated for one hour at room temperature with the primary IL-33 antibody (monoclonal mouse, anti-human, ALX-804-840-C100, 1:800, ENZO Life Sciences, U.S.A.), diluted in 1% BSA/PBS. Slides were incubated with biotin labeled polyclonal rabbit anti-mouse (E0413, 1:100, Dako, Denmark), diluted in 1% human serum + 1% BSA/PBS, before incubation with Streptavidin (Alexa Fluor™ 555 conjugate, S21381, 1:300, Alexa Fluor™, U.S.A.) diluted in diluted in 1% human serum + 1% BSA/PBS. Autofluorescence was blocked for 3 minutes using Vector® TrueVIEW® Autofluorescence Quenching Kit (SP-8400, Vector Laboratories, Canada) before cell nuclei were stained through incubation with DAPI (D9542, 1:1000, Sigma-Aldrich, U.S.A.) for 15 min at RT. VECTASHIELD Vibrance® Antifade Mounting Medium, provided with the TrueVIEW® kit, and coverslips were applied on the slides. At last slides were scanned at 20x magnification using SLIDEVIEW VS200 (Olympus Corporation, Japan).

Analysis of fluorescence double staining

Scans were imported in QuPath software, after which airways were cut out for analysis. Next, cell detection was performed in the airways using Stardist as a detection model for cell nuclei. In R software V.4.0.0 (Boston, Massachusetts, USA), cytoplasmic intensity values for IL-33 and p40 were used as a way of background correction, because both IL-33 and p40 are specifically expressed in nuclei and not cytoplasm. After background correction, per airway the cells were arranged and plotted from lowest to highest value in a histogram and a linear model was created to fit the curve of the plot. Once staining intensity in the cells increased exponentially, and cells thus did not match the linear model, they were marked as positive for the protein stained. Using this method, the total numbers of p40 and IL33 positive cells were

counted for each of the selected airways, and then the fraction of p40+ cells per airway that were also positive for IL-33 was calculated. Only airways with more than eight basal cells were used for analysis, which led to the exclusion of 2 patients because no large enough airways were present. The results derived from the analyses were tested for significant differences between the four different groups using linear mixed model analysis in R software V.4.0.0 (Boston, Massachusetts, USA).

Western blotting

For western blot, snap frozen lung tissue from resected lung tissue was used from current (n=10) and ex-smoker (n=9) COPD patients. Approximately 10 slices of 10µm were cut for the lung tissue samples and collected in RIPA Lysis and Extraction buffer (89900, Thermo Scientific™, U.S.A.) and Halt™ Protease and Phosphatase Inhibitor Single-Use Cocktail (100X) (1861281, 1x, Thermo Scientific™, U.S.A.). To assure tissue degradation and lysis of all cells, the tissue samples were run in Bullet Blender® Gold (Next Advance, U.S.A.) for 1 minute on speed 8, using 0,2 mm stainless steel balls. After tissue samples, but not the beads, were put in new cups, samples were centrifuged (Eppendorf Centrifuge 5417 R) for 10 minutes at 4°C and 10.000 RPM. Protein assay was performed using Pierce™ BCA Protein Assay Kit (23227, Thermo Scientific™, U.S.A.), where the standard curve was determined using Pierce™ Bovine Serum Albumin Standard Ampules (23209, Thermo Scientific™, U.S.A.). Absorbance was measured with CLARIOstar Plus (BMG Labtech, Germany). Absorbance was converted to protein levels, which was then used to take 25µg per sample, and adjust the volume to 20µl using the RIPA buffer after which 5µl loading dye was added. These samples were heated for 5 minutes at 100 °C, before resting on ice and pipetting 20µl per sample in 12.5% SDS-polyacrylamide gels. Electrophoresis was run at 100V, before blotting proteins on 0.45µm nitrocellulose membranes for 75 minutes at 4 °C and 100V. After blotting, images of the membranes were taken with Gel Doc™ EZ Imager (Bio-Rad Laboratories, U.S.A.) to visualize protein loading, before blocking with 5% ELK in TBST for 1 hour. Membranes were incubated at 4 °C overnight with the primary IL-33 antibody (AF 3625, 1:1000, R&D Systems, U.S.A.), followed by incubation with a HRP labeled rabbit anti-goat antibody (p0449, 1:1000, Dako, Denmark). The antibodies were visualized with SuperSignal™ West Pico PLUS Chemiluminescent Substrate (34578, Thermo Scientific™, U.S.A.), before blots were imaged/visualized with Invitrogen iBright 1500 (Thermo Scientific™, U.S.A.). After stripping for 10 min with stripping buffer, membranes were blocked again with 5% ELK in TBST before

incubation with an anti-beta actin antibody (ab 8227, 1:6000, abcam, U.K.) for one hour at room temperature. After incubation with an HRP labeled goat anti-rabbit antibody (P0448, 1:1000, Dako, Denmark), Pierce™ ECL Western Blotting Substrate (32106, Thermo Scientific™, U.S.A.) was used to visualize antibody binding. Images of the bands were taken with Invitrogen iBright 1500 (Thermo Scientific™, U.S.A.).

Western blot analysis

Normalization of samples was performed using β -actin expression. In iBright Analysis Software, protein bands associated with IL-33 and the splice variants (31kDa, 20kDa, 16kDa) and b-actin were analyzed using local background corrected density, after which the ratios of IL-33/b-actin were calculated for each sample and each of the IL-33 bands. Statistical analysis between groups were performed using Mann-Whitney U tests in Prism 8.0.1 (Graphpad Software inc, U.S.A.).

Table S1: Baseline characteristics of additional studies

Study	Sample Types	Smoking Status	n (%)	Mean Age (SD)	Gender male n(%)	Mean Pack years (SD)	Mean FEV1 % (SD) Prediction	Mean FEV1/FVC (SD)	Platform	Profiling Assay
TIP study(1)	Bronchial brushings	Current smokers	63 (100)	40.8 (19.2)	49 (78)	17.6 (16.8)	95.6 (20.5)	74 (14)	Microarray	Affymetrix HG 1.0 ST microarrays
Bulk RNA-seq in-vitro study (2)	Primary bronchial epithelial cells differentiated in Air-liquid interface	1/3/4 (non/ex/current smokers)	8	66.6 (6.2)	7(87.5)	N/A	N/A	68.9 (11.7)	Bulk RNA-Seq	Illumina NovaSeq6000 sequencer
GSE8545 Small airways Microarray (3)	Bronchial brushings of small airway epithelial cells	Current Smokers (non-COPD)	18 (33.3)	46 (5)	12 (66.7)	31 (16)	109 (15)	82 (5)	Microarray	Affymetrix Human Genome U133 Plus 2.0 Array
		Current Smokers (COPD)	18 (33.3)	50 (6)	15 (83.3)	34 (17)	82 (18)	64 (6)		
		Never Smokers	18 (33.3)	41 (7)	14 (77.8)	0	106 (9)	82 (5)		

Figure Legends

Figure S1. Normalized *IL1RAP* expression levels in bronchial datasets. **A** *IL1RAP* expression levels from the STOP study of bronchial biopsies (n=16) pre and post 12 months smoking cessation. **B** *IL1RAP* expression levels of bronchial biopsies from the GLUCOLD study of ex-smokers (n=33) and current smoker (n=46) COPD patients. **C** *IL1RAP* expression levels of bronchial brushes from the COPD microarray study of ex-smokers (n=57) and current smokers (n=30) COPD patients (GSE37147). **D** *IL1RAP* expression of bronchial biopsies from the NORM study of never (n=40) and current (n=37) healthy smokers. **E** *IL1RAP* expression of bronchial biopsies from the CRUKPAP study of never (n=8), ex- (n=151) and current (n=77) smokers. All analyses were corrected for age and gender. The numbers shown are p-values taken from results of differential expression analyses. Error bars are representing the standard deviation.

Figure S2. *IL33* and related genes expression in small airways samples. Expression of A) *IL-33* B) *IL1RL1* and C) *IL1RAP* in microarray data of small airway epithelium (GSE8545, 18 never smokers, 18 non-COPD current smokers and 18 COPD current smokers). Non-COPD [black] and COPD current smokers [green] data were merged. P-values shown on the figure were calculated from differential gene expression analysis using the limma R package which was corrected for age and gender.

Figure S3. Expression of *IL-33* after acute cigarette smoke exposure. **A** Expression of *IL-33* in a longitudinal dataset of bronchial brushings collected following 24 hours smoking cessation versus 24 hours after smoking 3 cigarettes. **B** Expression of *IL-33* in primary bronchial epithelial cells (n=8 donors) differentiated air-liquid interface were exposed to cigarette smoke or air for 24h. The error bar indicates the standard deviation. Gene expression was not significant between air and cigarette smoke exposure in any of the time points. **C** *IL-33* gene expression derived from bronchial biopsies from ex- (n=151) and current (n=77) smokers separated by their rs992969 genotype. P-values were acquired from Mann-Whitney for unpaired analyses.

Figure S4. Association between smoking and *IL1RL1* variants. A) Ratio of membrane and common (soluble and membrane) variant of *IL1RL1* in the COPD ex (n=18) and current smokers (n=38) (GLUCOLD study) and the normalized gene expression (CPM normalization) of *IL1RL1* variants: B) membrane and C) common (soluble and membrane) variant. D) Ratio of membrane and common (soluble and membrane) variant of *IL1RL1* in healthy never (n=40) and current smokers (n=37) and the gene expression of both E) membrane and F) common (soluble and membrane) variant (NORM study).

Figure S5. Single cell analysis of Human Lung Cell Atlas.

Violin plots of **A** *IL-33* and **B** *IL1RL1* in cell derived from nasal, bronchial and lung samples of the Human Lung Cell Atlas 1.0.

Figure S6. Summary of why anti-*IL-33* treatment is more effective in ex- smokers than compared to current smokers. Higher number of basal cells at the pre-differentiation state where *IL-33* is primarily expressed in ex- smokers (right) than current smokers (left). Images were acquired from Servier Medical Art by(<https://smart.servier.com/>)

References

1. Billatos E, Faiz A, Gesthalter Y, LeClerc A, Alekseyev YO, Xiao X, et al. Impact of acute exposure to cigarette smoke on airway gene expression. *Physiological Genomics*. 2018;50(9):705-13.
2. Wohnhaas CT, Gindele JA, Kiechle T, Shen Y, Leparo GG, Stierstorfer B, et al. Cigarette Smoke Specifically Affects Small Airway Epithelial Cell Populations and Triggers the Expansion of Inflammatory and Squamous Differentiation Associated Basal Cells. *Int J Mol Sci*. 2021;22(14).
3. Ammous Z, Hackett NR, Butler MW, Raman T, Dolgalev I, O'Connor TP, et al. Variability in Small Airway Epithelial Gene Expression Among Normal Smokers. *Chest*. 2008;133(6):1344-53.
4. Shabalina AA. Matrix eQTL: Ultra fast eQTL analysis via large matrix operations. *Bioinformatics* 2012;28(10):1353-8.
5. Aneas I, Decker DC, Howard CL, Sobreira DR, Sakabe NJ, Blaine KM, et al. Asthma-associated variants induce *IL33* differential expression through a novel regulatory region. *bioRxiv*. 2020:2020.09.09.290098.
6. Grotenboer NS, Ketelaar ME, Koppelman GH, Nawijn MC. Decoding asthma: translating genetic variation in *IL33* and *IL1RL1* into disease pathophysiology. *Journal of allergy and clinical immunology*. 2013;131(3):856-65. e9.
7. Imkamp K, Berg M, Vermeulen C, Heijink I, Guryev V, Koppelman G, et al. Comparison of gene expression profiles from nasal and bronchial brushes. *European Respiratory Journal*. 2017;50(suppl 61):OA2910.
8. Ketelaar ME, Portelli MA, Dijk FN, Shrine N, Faiz A, Vermeulen CJ, et al. Phenotypic and functional translation of *IL33* genetics in asthma. *Journal of Allergy and Clinical Immunology*. 2021;147(1):144-57.
9. Li X, Hastie AT, Hawkins GA, Moore WC, Ampleford EJ, Milosevic J, et al. eQTL of bronchial epithelial cells and bronchial alveolar lavage deciphers GWAS-identified asthma genes. *Allergy*. 2015;70(10):1309-18.
10. Aliee H, Massip F, Qi C, Stella de Biase M, van Nijnatten JL, Kersten ETG, et al. Determinants of SARS-CoV-2 receptor gene expression in upper and lower airways. *medRxiv*. 2020:2020.08.31.20169946.
11. Newman AM, Liu CL, Green MR, Gentles AJ, Feng W, Xu Y, et al. Robust enumeration of cell subsets from tissue expression profiles. *Nature Methods*. 2015;12(5):453-7.
12. Badi YE, Salcman B, Taylor A, Rana B, Kermani NZ, Riley JH, et al. *IL1RAP* expression and the enrichment of *IL-33* activation signatures in severe neutrophilic asthma. *Allergy*. 2023;78(1):156-67.
13. Hänzelmann S, Castelo R, Guinney J. GSEA: gene set variation analysis for microarray and RNA-Seq data. *BMC Bioinformatics*. 2013;14(1):7.
14. Faiz A, van den Berge M, Vermeulen CJ, Ten Hacken NH, Guryev V, Pouwels SD. *AGER* expression and alternative splicing in bronchial biopsies of smokers and never smokers. *Respiratory Research*. 2019;20(1):1-4.

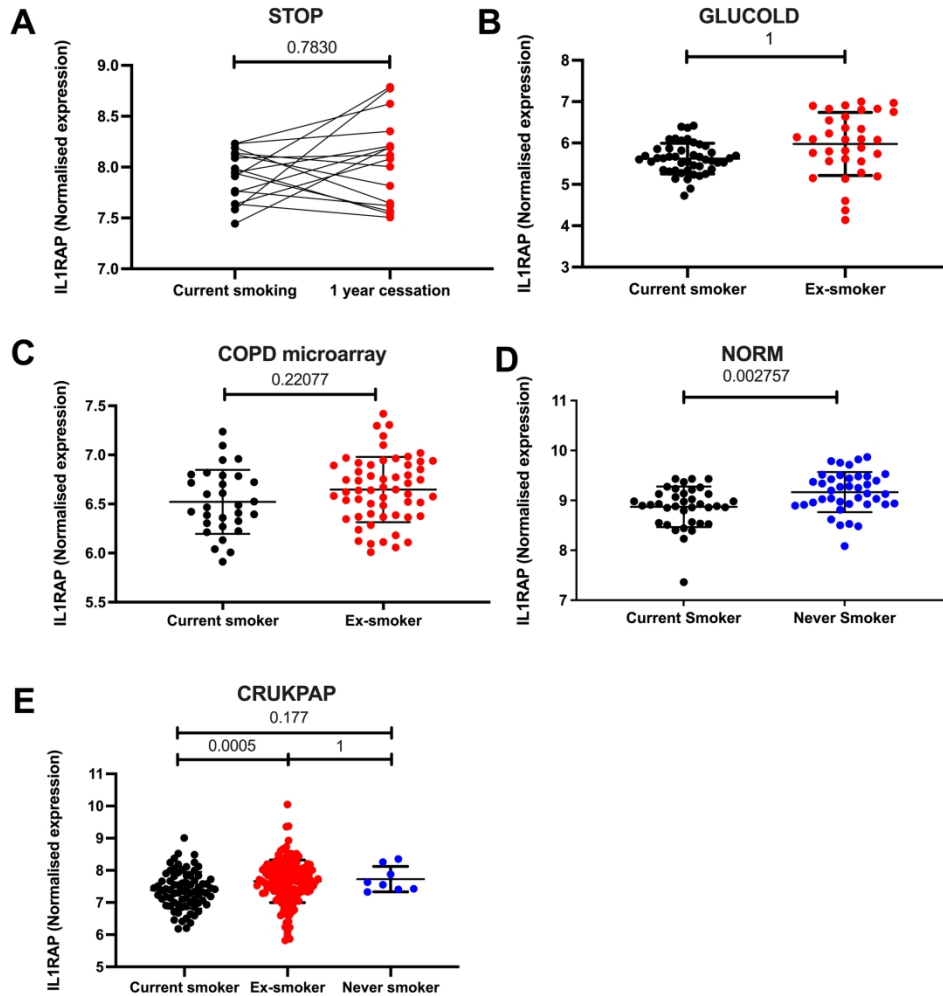


Figure S1. Normalized IL1RAP expression levels in bronchial datasets. A IL1RAP expression levels from the STOP study of bronchial biopsies (n=16) pre and post 12 months smoking cessation. B IL1RAP expression levels of bronchial biopsies from the GLUCOLD study of ex-smokers (n=33) and current smoker (n=46) COPD patients. C IL1RAP expression levels of bronchial brushes from the COPD microarray study of ex-smokers (n=57) and current smokers (n=30) COPD patients (GSE37147). D IL1RAP expression of bronchial biopsies from the NORM study of never (n=40) and current (n=37) healthy smokers. E IL1RAP expression of bronchial biopsies from the CRUKPAP study of never (n=8), ex- (n=151) and current (n=77) smokers. All analyses were corrected for age and gender. The numbers shown are p-values taken from results of differential expression analyses. Error bars are representing the standard deviation.

202x205mm (300 x 300 DPI)

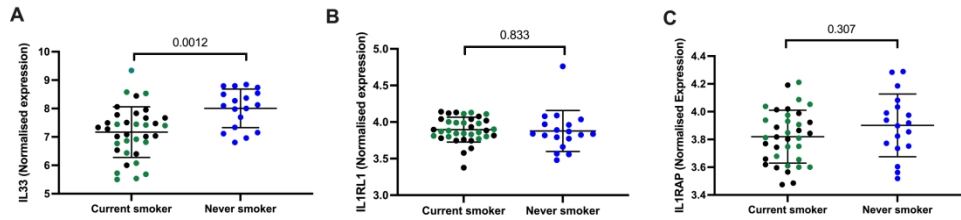


Figure S2. IL33 and related genes expression in small airways samples. Expression of A) IL-33 B) IL1RL1 and C) IL1RAP in microarray data of small airway epithelium (GSE8545, 18 never smokers, 18 non-COPD current smokers and 18 COPD current smokers). Non-COPD [black] and COPD current smokers [green] data were merged. P-values shown on the figure were calculated from differential gene expression analysis using the limma R package which was corrected for age and gender.

287x65mm (300 x 300 DPI)

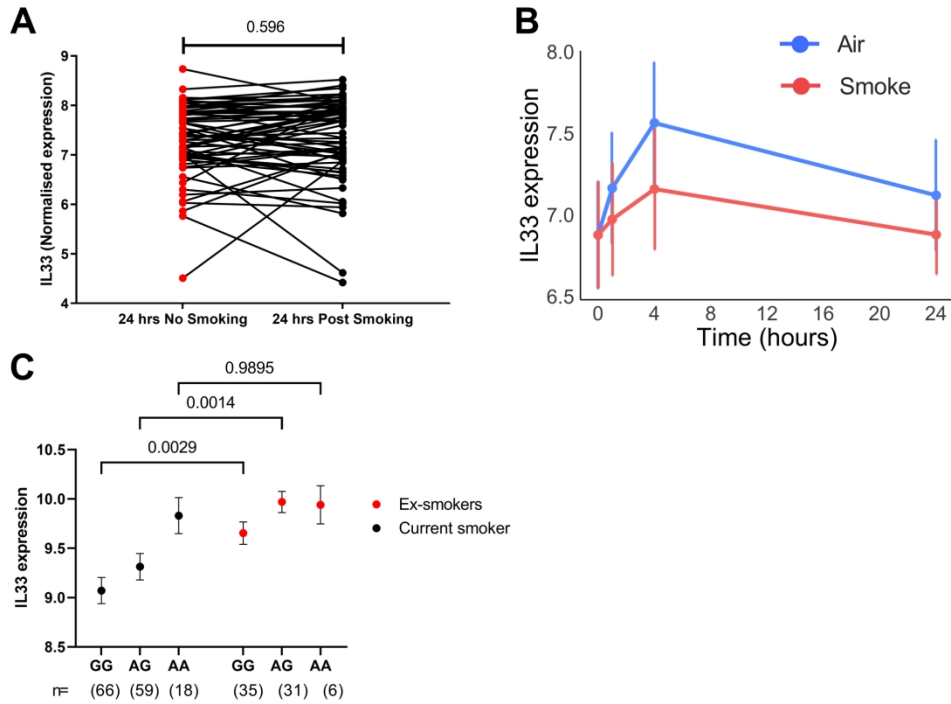


Figure S3. Expression of IL-33 after acute cigarette smoke exposure. A Expression of IL-33 in a longitudinal dataset of bronchial brushings collected following 24 hours smoking cessation versus 24 hours after smoking 3 cigarettes. B Expression of IL-33 in primary bronchial epithelial cells (n=8 donors) differentiated air-liquid interface were exposed to cigarette smoke or air for 24h. The error bar indicates the standard deviation. Gene expression was not significant between air and cigarette smoke exposure in any of the time points. C IL-33 gene expression derived from bronchial biopsies from ex- (n=151) and current (n=77) smokers separated by their rs992969 genotype. P-values were acquired from Mann-Whitney for unpaired analyses.

194x145mm (300 x 300 DPI)

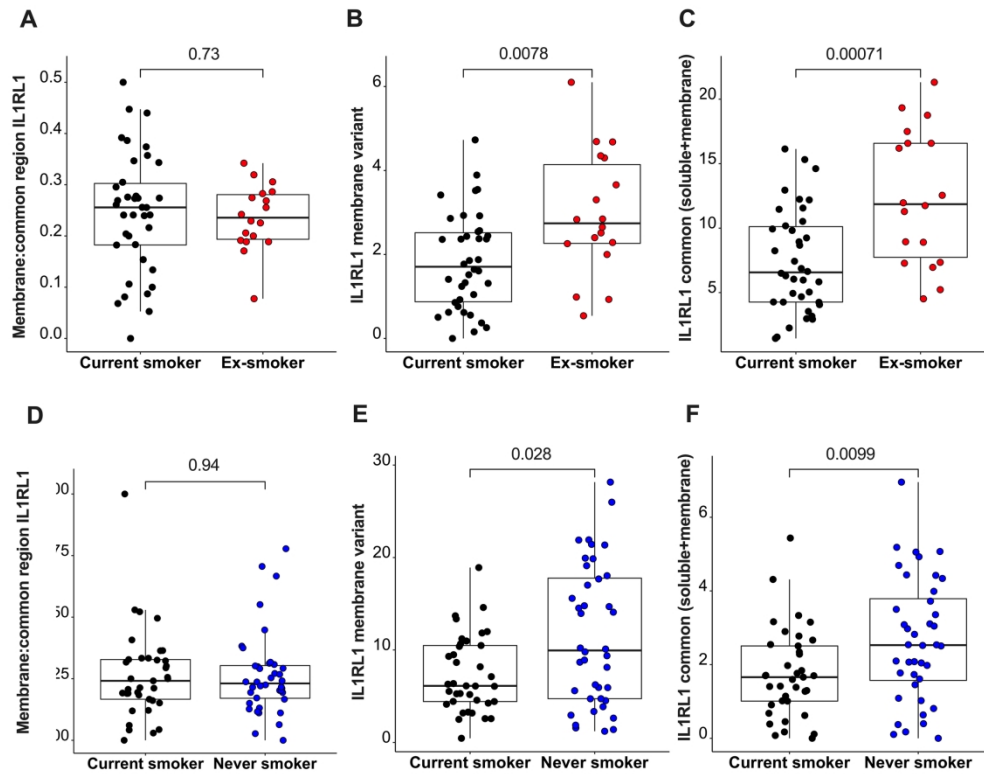


Figure S4. Association between smoking and IL1RL1 variants. A) Ratio of membrane and common (soluble and membrane) variant of IL1RL1 in the COPD ex (n=18) and current smokers (n=38) (GLUCOLD study) and the normalized gene expression (CPM normalization) of IL1RL1 variants: B) membrane and C) common (soluble and membrane) variant. D) Ratio of membrane and common (soluble and membrane) variant of IL1RL1 in healthy never (n=40) and current smokers (n=37) and the gene expression of both E) membrane and F) common (soluble and membrane) variant (NORM study).

233x185mm (300 x 300 DPI)

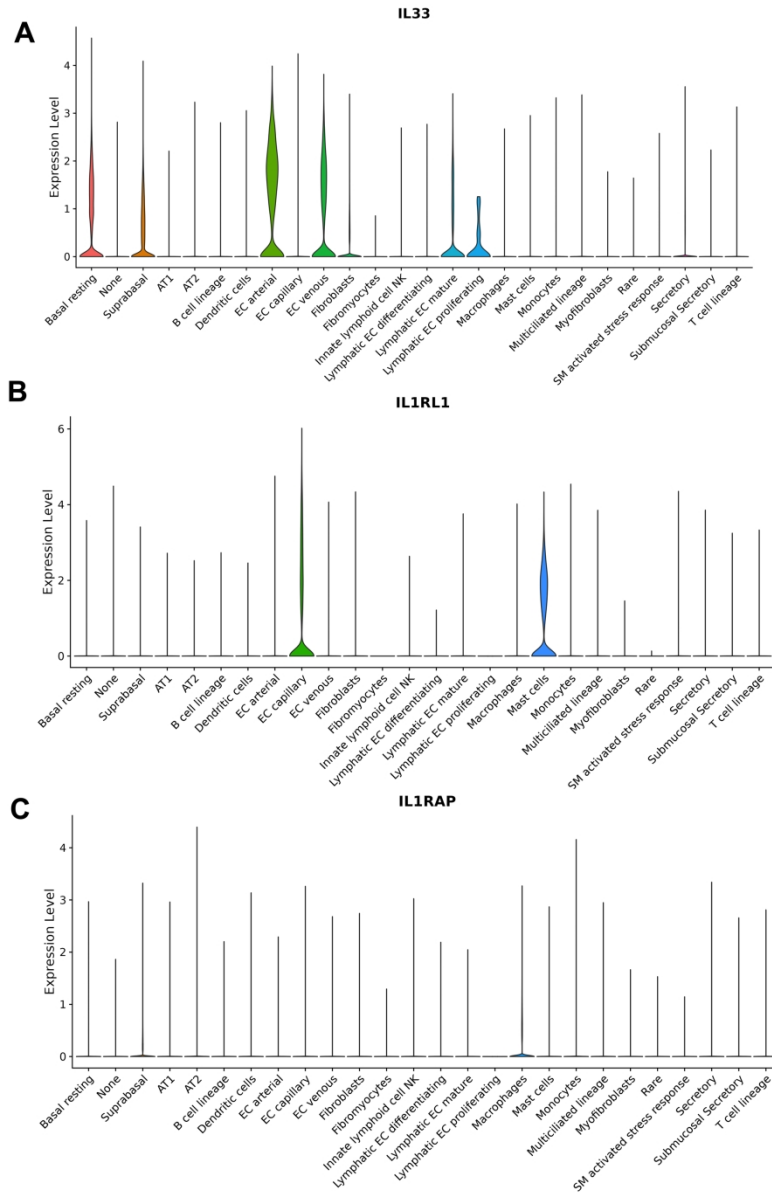


Figure S5. Single cell analysis of Human Lung Cell Atlas. Violin plots of A IL-33 and B IL1RL1 in cell derived from nasal, bronchial and lung samples of the Human Lung Cell Atlas 1.0.

194x294mm (300 x 300 DPI)

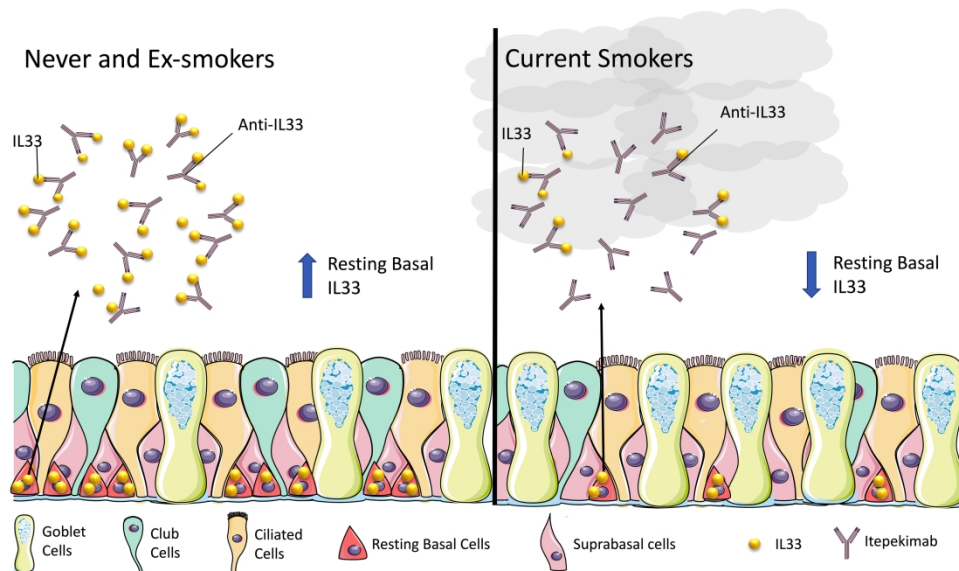


Figure S6. Summary of why anti-IL-33 treatment is more effective in ex- smokers than compared to current smokers. Higher number of basal cells at the pre-differentiation state where IL-33 is primarily expressed in ex- smokers (right) than current smokers (left). Images were acquired from Servier Medical Art by(<https://smart.servier.com/>)

297x169mm (300 x 300 DPI)